Solrheat Solar Heater

INSTALLATION AND TESTING REPORT, JULY 2016

M.G. Evans and C.M. Asciak
UNIVERSITY OF NEW ENGLAND | ASCIAK SOLAR AIR HEATING

Introduction

The Solrheat® solar heater is an innovative high-output, high-efficiency solar heat exchanger designed for domestic and commercial heating. The heater operates in the range of solar conditions experienced in a typical NSW winter, producing reliable heating from light overcast to full sun at a low operating cost. The system was designed and tested by a team working in the New England region of NSW.

The heater is a roof-installed ducted heat absorption panel, 1 x 2 m profile, powered by an 80-watt mixed flow fan and controlled by a thermostat combining internal and external temperatures. The heater produces an average of between 600 and 1000 watts of heated airflow in design winter conditions, the lower value corresponding to light overcast conditions. Peak heating rates occurs between 11 am and 1pm, typically reaching 1100 to 1500 watts at peak.

The heater is highly efficient, converting up to 80% of total solar power directly to heat. Input efficiencies as high as 90% are based on realistic solar absorption plus electric fan inputs.

Heat flow is greatly reduced in severe overcast. The heater is inoperable at night.

Net daily heating varies between 4.6 and 8.5 kWh, or 8.3 to 15.3 MJ/day per square metre of solar collecting surface. This compares very favourably to net insolation data in the range of 8 to 16 MJ/m^2/day at a horizontal ground surface in Armidale in the winter months.

The following test report outlines the test procedure and results, and includes a calibrated theoretical model that can be applied to forecast heater performance in a range of weather and operating conditions. Installation can be designed to maximise available light and sources of warm air in the building. Operating air flow rates can be matched to installation and climate variables. The control thermostat can be set to smaller or larger temperature differences.

A significant observational result of the installation testing is that it is possible to significantly increase the temperature of heated air by turning the fan and heater flow rate down. This reduces the net heat flow slightly but significantly improves the temperature gain, as well as reducing the running cost of the fan. This inverse operating rule is visible in the experimental results and is explained by the theoretical analysis.

A second finding is that a heater may operate at a very high power for up to 15 minutes if allowed to warm up in the morning-noon peak. This appears to prime the heater with a quantity of stored heat that can be used to significantly warm a house in the early afternoon or on low-sun days warm a smaller space such as a workroom or drying room.

Home or Business Heating

The heating benefit of a solar heat flow depends on the house volume to be heated and the insulation characteristics of the building as well as the preferences of the household or business. There are two heater performance characteristics that can be optimised to suit the building's characteristics: The heater power output (in watts or kWh), and the temperature gain, that is the increase in temperature between cool inflow and warm outflow.

The temperature gain can be increased by turning the flow rate and heater power down. Slow-flowing air resides longer in the heater exchanger and warms to a higher temperature. The

lower flow rate results in a slight reduction in heater power, leading to the familiar trade-off of a smaller space that can more easily be kept at a higher temperature.

Heater power gives a good indication of system performance in that it combines the temperature gain with the quantity of air heated. The temperature gain on the other hand is an indication of sensible warmth that is often inverse to the heater power, but corresponds more closely to the user's sense of warmth.

Temperature response is not immediate, but a change to a new temperature setting can be felt within a few minutes and adjusted for the best sense of comfort in warmth and airflow. The heater provides sustained heating, typically between 25 and 30^{o}C at around 80 litres per second or 288 cubic metres per hour.

Warmer airflow is slightly less efficient but is compensated by the decreasing electrical cost of the fan. The temperature gain can be regulated anywhere between +5^{o}C and +20^{o}C, with consideration of the smaller space heating of the higher temperatures.

At very high flow rates the temperature gain may reduce to only a few degrees, limiting the effectiveness of heating despite extracting a large proportion of the available solar power. Conversely at very low flow rates the temperature gain is large but may fail to circulate through a building, hence again negligible effective heating. Optimal performance involves finding an appropriate balance between these two extremes.

Experimentation is useful for determining a building's best flow control settings. An optimum setting can be left in place for general use. Low settings can improve performance in overcast conditions and in morning / afternoon light. High settings should be used only at the peak of fine winter days.

An estimate can be made by considering the volume that can be warm-cycled in a two-hour peak period of the day: in cubic meters this is the fan flow rate multiplied by 60 x 60 x 2 = 7200 seconds. Floor plan can be estimated by reducing this value for a 2.4 m standard ceiling height:

$$\text{Room Area } (m^2) = 7200\ (s) \times Q\ (m^3/s) \div 2.4\ (m) = 3 \times Q_{wrm}\ \text{(litres/second)}$$

Q_{wrm} is the warm air flowrate in litres/second, on a range between 20 and 120 l/s. The area that can be heated is that value multiplied by 3. For a given temperature gain such as 10^{o}C the heated area increases with available sunlight, from around 60 m^2 to 360 m^2 in the solar 200 – 900 W/m^2 range. In addition to flowrate control, variable space heating is a viable strategy, by opening more rooms to the warm airflow as the sun emerges.

Inlet and Outlet Installation

The system operates best when warm air in the building is tapped by a cool inlet duct at a large distance from the warm outlet duct. It is important to ensure that the cool inlet duct is not "short-circuited" by taking warm air directly from the warm outlet area. A long flowpath improves uniformity of heating in a main corridor of the whole house. A warm temperature at the cool intake is preferred since this can be heated by the same gain to a higher actual temperature, giving the warmest outflow for any setting.

Cool inlets may be formed into walls, feature risers. The optimum inlet is likely to be low on a north aspect internal wall since by day in operation these will be the warmest spaces in a house.

Intake and outlet ducts should form a closed circuit with the fan and heater. There are issues with circulation and insulation that must be addressed in every case. Low-level cool inlets are likely to give the best combination of distance and cool temperature in operation. High outlets promote air movement downwards, mixing warm air more uniformly.

Warm outlets should be positioned in rooms that will be most in use by day, such as work rooms or living rooms. A warm outlet in a bedroom provides a comfortable play room or sick room. The first room in the air circuit becomes the warm room on overcast days when flow rate is turned down to provide temperature gain in the smaller space.

A number of commercial systems are designed to circulate roof space air with dust filtration to provide an economical source of warm daytime air. A roof-mounted heater can enhance this by drawing intake air from the roof space air and adding solar heating to that input, so long as this circulates with the closed warm air cycle in the building.

The roof space may need to be sealed at the eaves for this to form a closed system, which would add to installation expenses for a roof space inlet.

Summer Night Cooling

Economical evening air conditioning can be produced by installing external vents on the fan line to bring in cool air and exhaust warm air. Radiative cooling by the plate is minor, certainly less effective than simply exhausting warm air via the ducted fan system.

10-Year Payback Period over +20-Year Operating Life

Continuous temperature gain and flow rate data obtained over 33 days of test operation provide an average heat energy flow of 6 kWh per day. This is close to the average insolation to a horizontal surface in this climate zone and accords with separate estimates of heater efficiency.

This heat output comes at an operating cost of 0.3 kWh per day for the 40 W fan over a typical 7-hour daylight operation period. The resulting net 5.7 kWh per day can be used to estimate a heat budget income by which the heater pays for itself.

Assuming a power input cost of 30 cents per kWh and a typical electrical-heat conversion efficiency of 100%, 5.7 kW/h per day represents an avoided cost of around $1.71 per day. Averaged over all weather conditions in a typical 8-month (240 day) Autumn-Spring period, the heater earns (by avoided cost) around $410 per year. At an installation cost of around $4000, this gives a payback period of around 10 years.

The heater can be assumed to have an operating life of over twenty years or indefinitely with expected replacement of electrical-mechanical components (fan, thermostat) every ten years.

Performance Graphs

The performance of the heater is best illustrated graphically. The following examples are selected from the experimental-analytic sections of this report to indicate ranges of typical behaviour. The graphs compare temperature gain, heater power and flowrate.

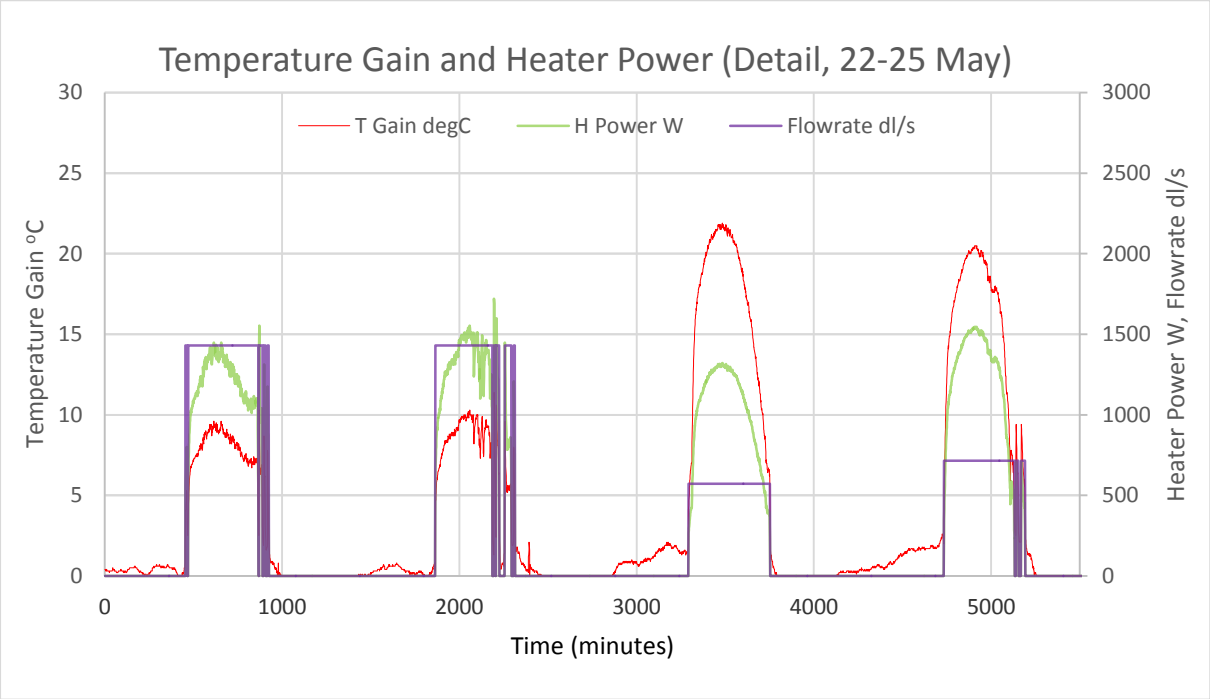

Figure 1: First four days of continuous analysis. Flowate is reduced and adjusted on days 3 and 4. Temperature gain increases from around 8° to around 20° while heater power is inverse averaging over 1100 Watts. Sunlight dips slightly in this period, morning-afternoon cloud day 1, light overcast day 2, good sunlight day 4. Periods of overcast are visible as on-off flow.

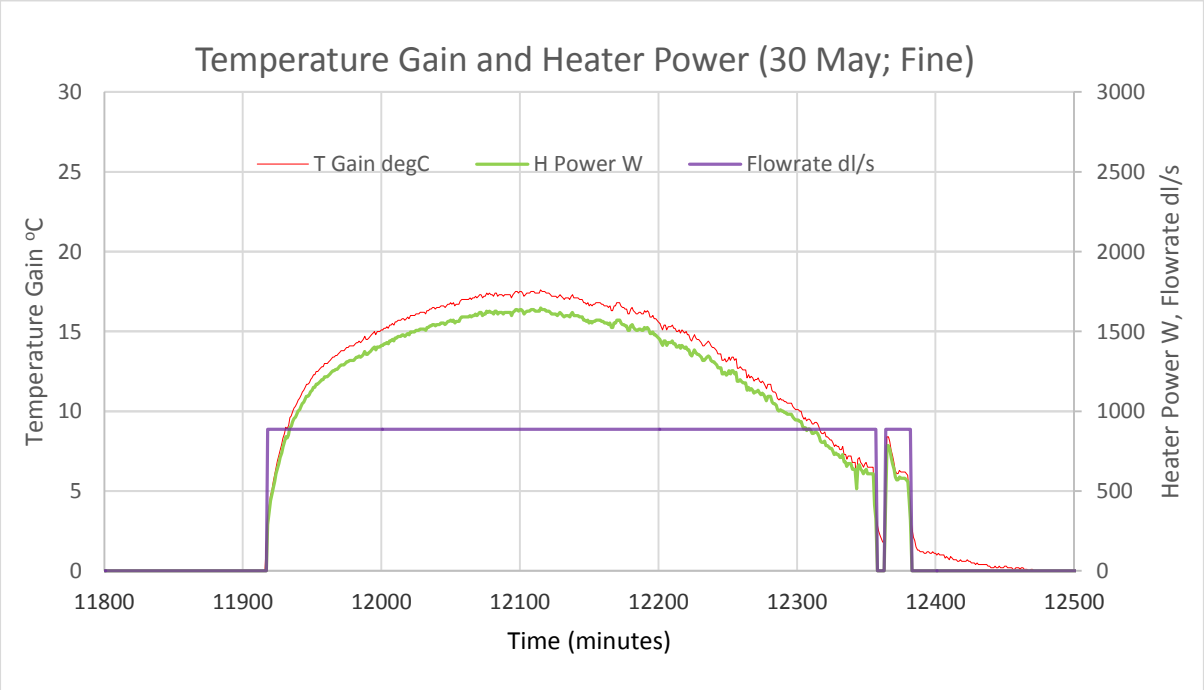

Figure 2: Detail of analysis for 30/5/2016. Warm weather and intermediate flowrate produced a very large heat output with high temperature gain. The flowrate at 89 l/s is not ideal, and could be improved by local experimentation.

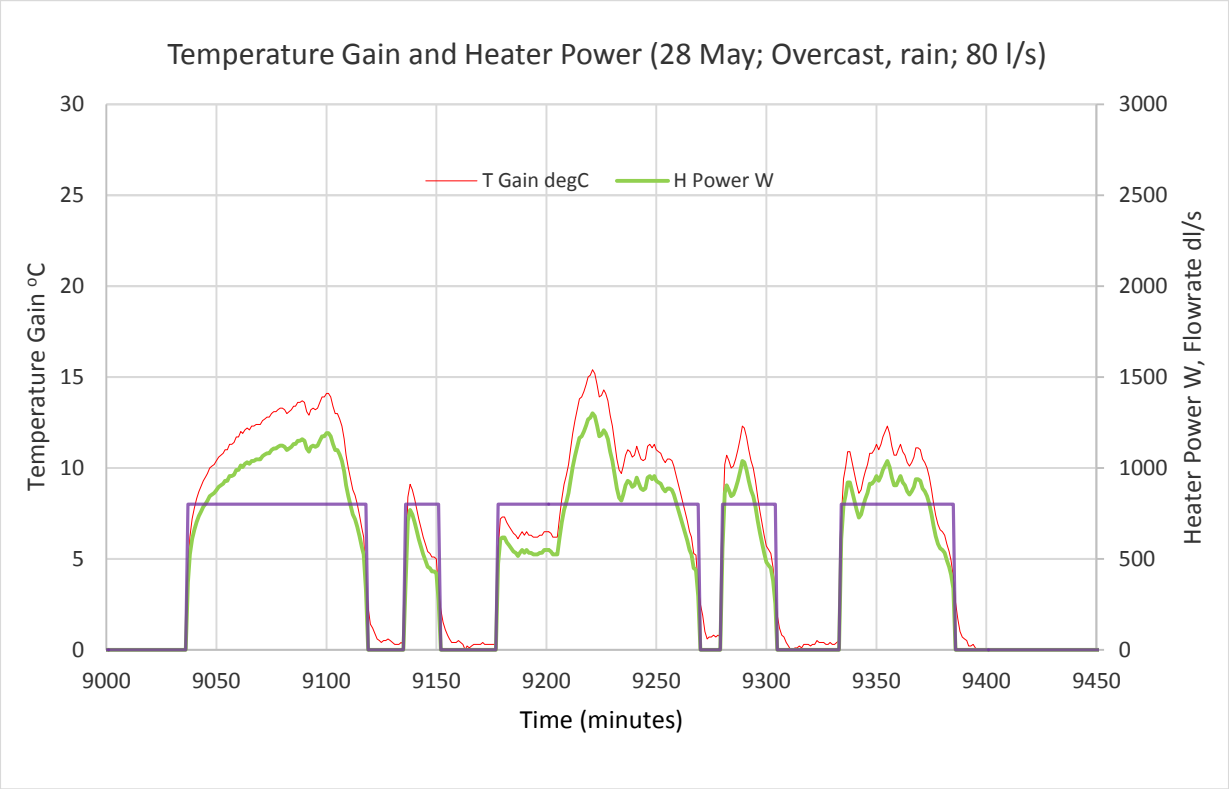

Figure 3: On-off operation should be avoided if possible by moderating the flow rate. Flow shown here could be reduced from 80 l/s to 70 l/s to prevent on-off.

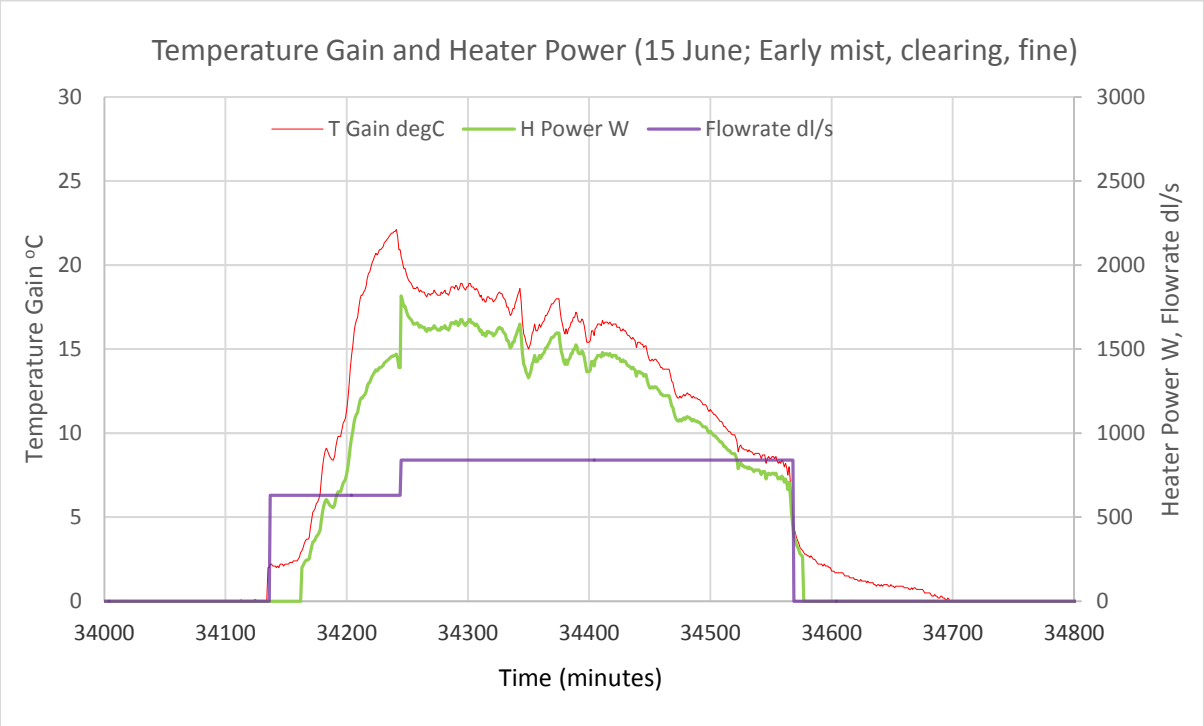

Figure 4: Detail of analysis for 15/6/2016. Early fog suggested a low flowrate, 63 l/s. Emerging sun suggested an 11am increase, to 84 l/s. The tendency to overgain the temperature at low flow in high sun is corrected and heater power increased.

Testing concluded with a test of heat priming of the installed system – the heater was left off in morning sun until 11:55 am, then run at a target optimum flow rate for the rest of the afternoon. The spike in temperature gain and heater is clearly visible in the graph – initial temperature gain of 65°C and 4200 W were strong departures from the moderate warm gains in conventional operation under thermostat control.

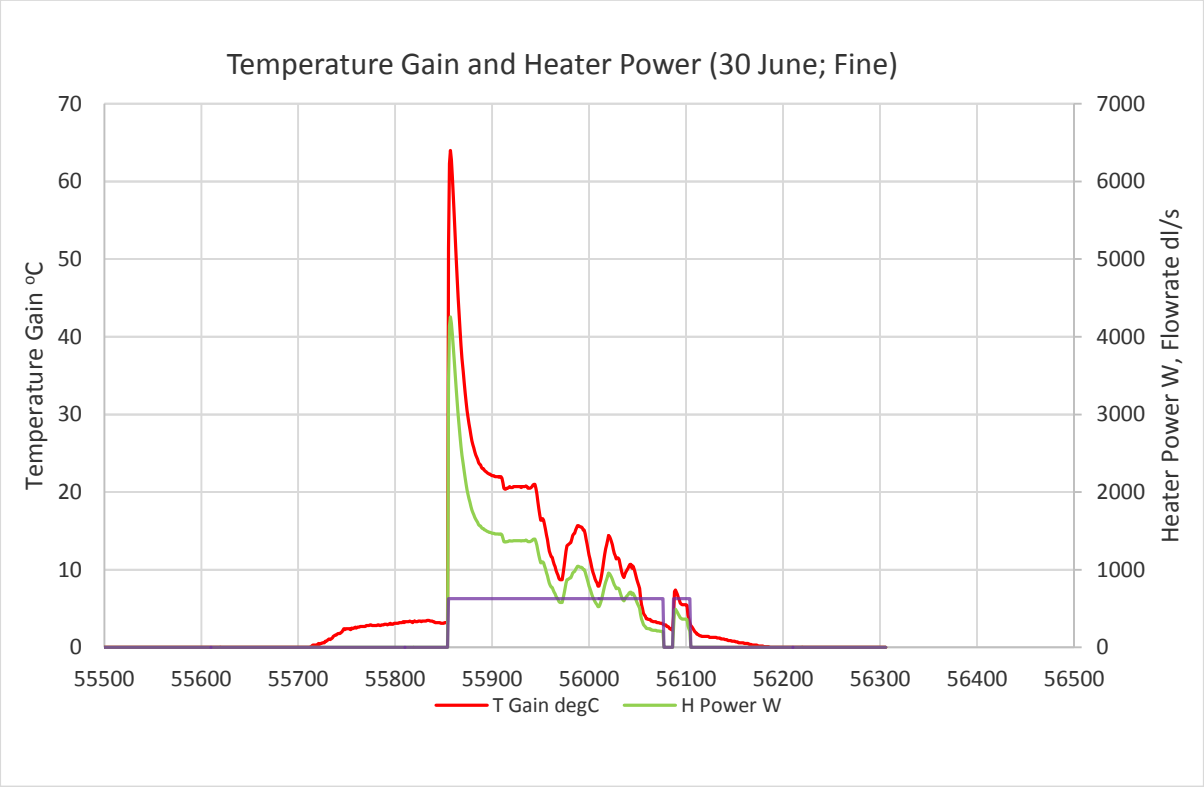

Figure 5: Detail of analysis for 30/6/2016. Heater off in in full sun to prime until 11:55, then on at 63 l/s. Peak temperature gain & power were 65 degrees at 4200 W. Output decreased to 22°C at 1400 W over one hour. This released 2.2 kWh in one hour, 4.4 kWh for the day. In volume-temperature terms, 226 m^3 were heated in one hour to a mixture temperature of 39°C. In a house, this would be far too warm for comfort but would significantly alter the building temperature well into late afternoon. It would be ideal for outlet into a drying room.

The theoretical model produce provides graphs of operation over a range of weather and operation variables, which are in general agreement with test data. The two main variables are sunlight and flowrate, which are co-varied and compared in Figures 6 and 7 below. These performance graphs can be used as a basis for optimum operation in any installation setting.

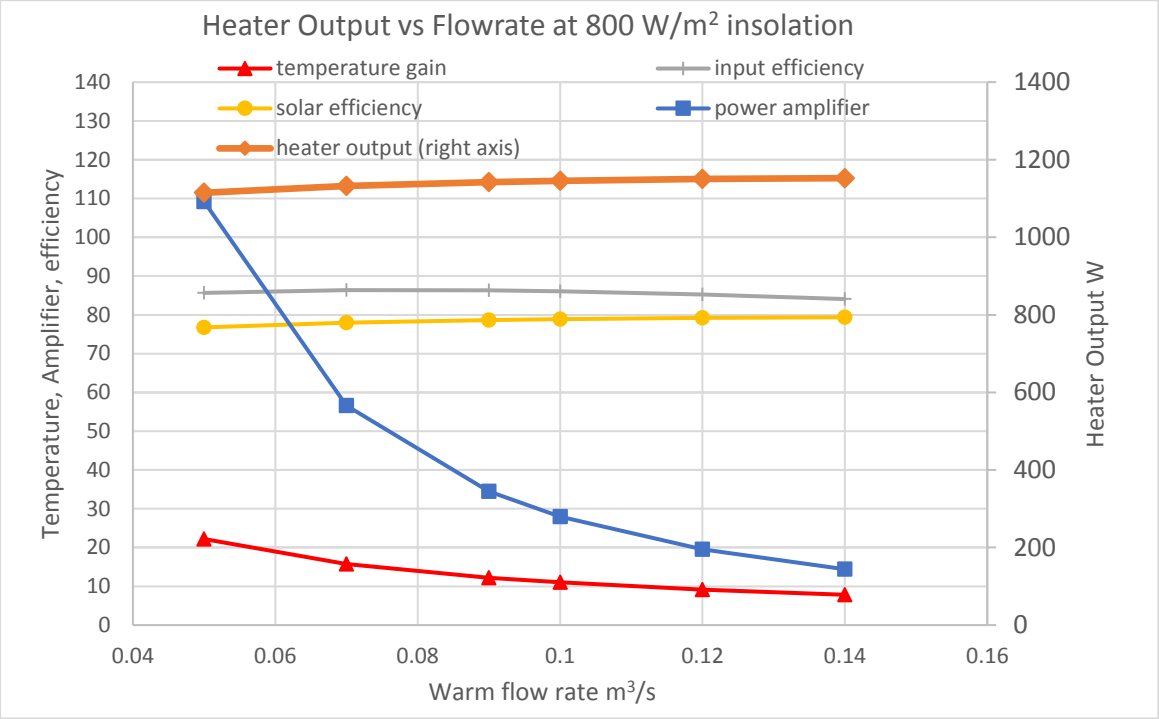

Figure 6: Heater power and temperature gain depend on flowrate, with optimum efficiency at flow rates around 70 – 80 litres per second.

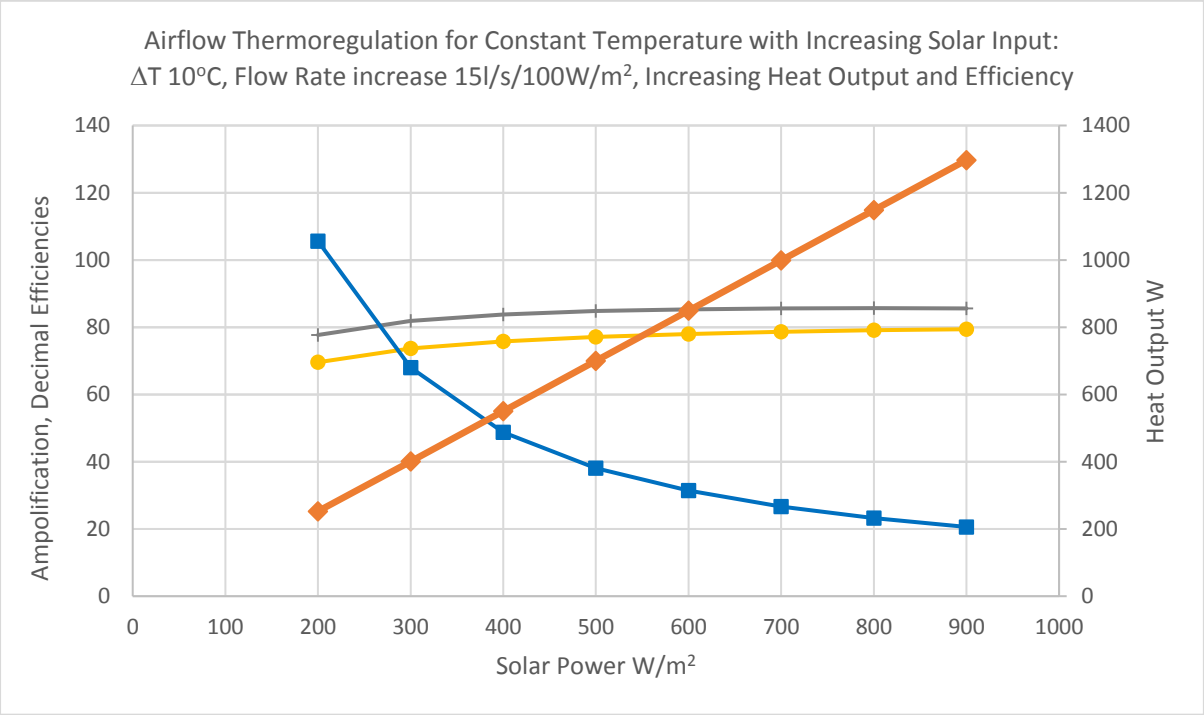

Figure 7: Thermoregulation at ΔT of 10°C *increasing flow rate* @15 *l/s /* 100 W/m² *insolation.*

Figures 6 and 7 examine heater performance with varying flowrate and insolation. In Figure 6 the flowrate is adjusted to show the range of temperature gain from 8°C to 22°C while heater power is nearly constant at 1100 W. Lower insolations are also examined in the report.

In Figure 7 the flowrate is adjusted to maintain a constant temperature gain of 10°C in response to variable insolation ranging from 200 to 900 W/m². Heater power increases from 250 W to 1300 W in this range. Efficiency increases as flow rate theoretically tracks available sunlight.

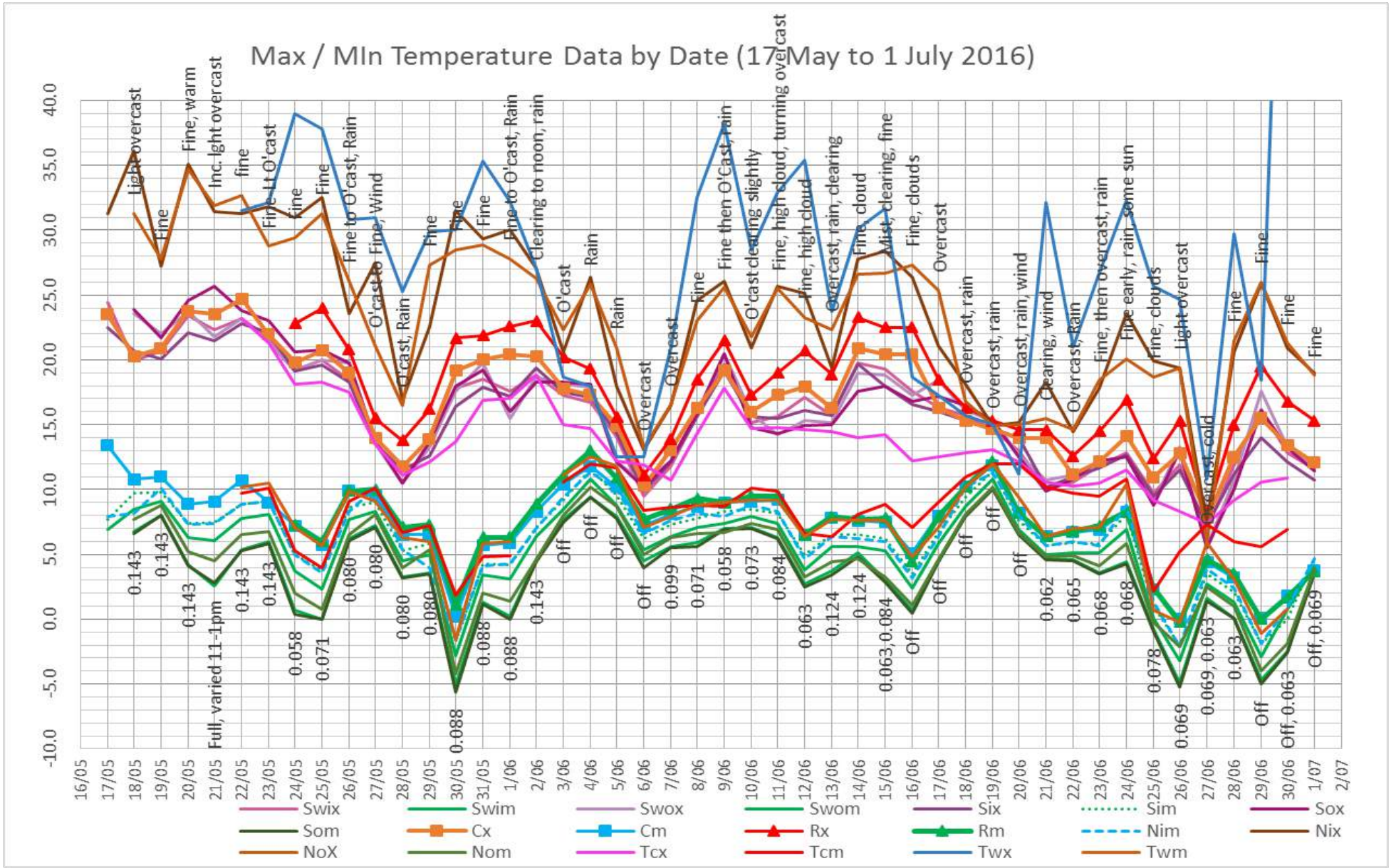

Figure 8: Graph of max/min building temperatures by date. The centre and ceiling positions (triangles, squares) are signifiantly warmer than the southern walls when the heater is running. The warm outflow temperature (blue) is consistently the warmest maximum temperature in the building, averaging 30°C. Labels show weather conditions and flow rate. There are visible correlations between flowrate and building temperature performance.

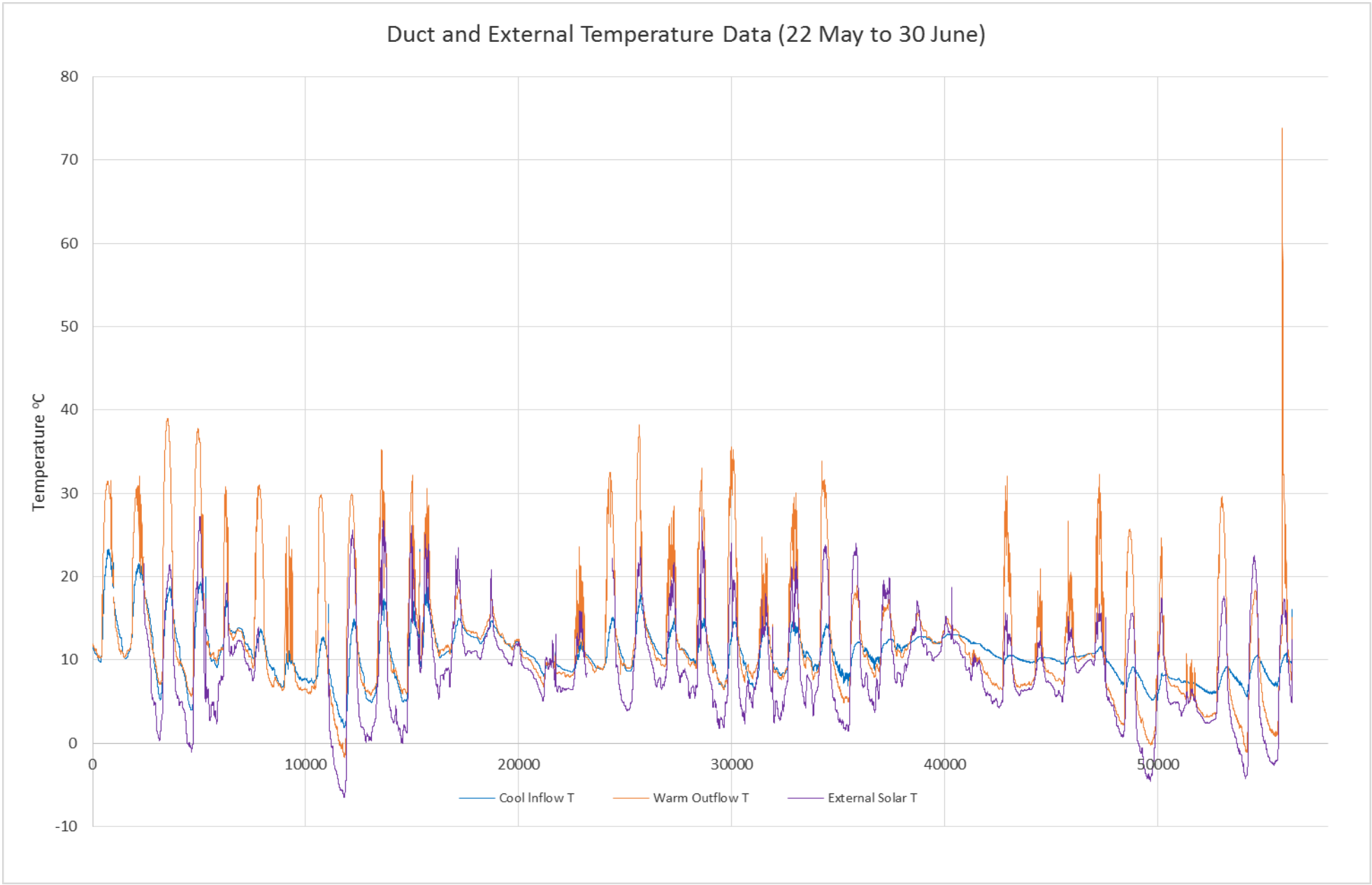

Figure 9: Continuous temperature data in cool and warm duct airflow, and external solar-ambient temperature. Dates are from 22 May to 30 Jun

Ducted Solar Heater: Experimental / Theoretical Analysis

The heater works by solar absorption onto a low-emission black solar-coated aluminium plate with extruded internal fins. Internal airflow produces a turbulent heat exchange process between the plate internal surface area and the airflow, subject to heat losses due to longwave thermal re-radiation from the external heating plate. There are small amounts of loss by conduction and convection from external glass and aluminium surfaces, small because these surfaces remain cool in operation.

Thermal flow rates in the heater are modelled by standard thermodynamic theory. The model is calibrated by thermometric measurements at key locations:

- Continuous inflow and outflow air temperatures (inflow/outflow ducts);
- Continuous ambient temperatures in sun-exposed and shaded locations.
- Discrete inflow and outflow plate temperatures (in/out ends of heater plate);
- Discrete temperature gradients on external glass and aluminium surfaces (five locations on the heater box and cover glass);
- Discrete internal and external temperatures at representative points in the test lab (South and North walls, 2 m and 4 m positions above centre of main workshop floor);

Discrete warm air outflow rates were also measured directly by hand-held anemometer (outflow duct). Discrete barometric and pyrometric observations were used to calibrate point efficiency estimates to air density and solar power.

Observations made in the pilot study ([1]2015) showed nearly equal temperature gradients along the heating plate and within the internal airflow. This suggested a simplification of the differential thermodynamic theory, leading to a bulk steady-state analytic model suitable for system design calculations aimed at identifying optimum operation.

The following analysis provides recommendations for adjustable flow rates given specific information on building dimensions and ambient climate conditions. The bulk model is in good agreement with the more detailed integral model ([2]2010) that was developed for prototype design calculations.

Data Design and Analysis

The test building is a 10 x 15 x 4m steel-framed aluminium-clad portal frame workshed, originally a farm mechanisation laboratory but now in use as a geology and soil science lab. The shed is insulated only under the roof and represents a challenge to any form of heating. A small central heating radiator positioned behind a storage cupboard is largely ineffective. Roof-mounted exhaust fans have an unknown effect on ventilation and cooling in the building.

This “tin lab” is suitable as an extreme test of the heating capacity of the system. If heating rates are found to be statistically significant and noticably more comfortable in this building, it will indicate a probability of effective heating in insulated homes and businesses. This is considered to be a second pilot study prior to testing within a domestic installation.

---

[1] Evans, MG 2015. *SolrHeat Space Heater Thermal Testing (Winter Design Conditions).* Test Report, Asciak Solar Air Heating.

[2] Evans, 2010. *Design Optimisation of Asciak Solar Heat Exchanger.* Design Report, Asciak Solar Air Heating

The heat exchanger was installed on ground outside the north wall of the building, ducting into the building through 6m of insulated 250mm ducting via a window panel at eye level. The panel was oriented north with good solar access between 8:30am and 4:30pm. Warm outflow duct entered horizontally into the building. The cool intake fan was in a filtered box under the adjacent workbench, pointing in a direction away from the warm outflow.

Continuous temperature data later found the cool intake to be consistently the coldest point in the room at maximum temperature. This tends to confirm that the cool intake was not effected by short-circuiting of warm air.

Four electronic resistance max/min thermometers were positioned at points along the south wall, north wall and in the centre of the building, with dual readings for inside/outside and ceiling/head height. Maximum and minimum daily temperatures were recorded at these 8 points. Simultaneous internal and external temperatures were also recorded.

This grid of daily observations was designed to give a cross-sectional daily temperature profile for the building and to provide comparisons of data to establish the degree of warming for different heater flow rates and when the heater is off.

Continuous datalogging thermometers recording at 1 minute intervals were installed in the cool inflow and warm outflow ducts. A third continuous thermometer was installed under a grass-green plastic tub in a sunlit spot a short distance from the heater. This was designed as a pyranometric thermometer showing warm-sun temperature or ambient temperature during periods of overcast, to indicate periods of sun and overcast as well as ambient night-time air temperatures. The heater exterior is typically cool, near ambient temperature. This cool temperature indicates effective insulation, resulting in a high efficiency.

The continuous thermometer data were used to calculate minute-by-minute temperature gains and heat flow rates and to correlate performance with periods of sunlight. Overnight the data were used to correlate cooling rates and derive thermal loss parameters for the building. Simultaneous inside/outside measurements during the evening cooling period were used to derive typical temperature differentials for heat loss.

Two 110^{o}C metal thermometers were introduced onto the external plate of the heater, providing point measurements of inflow and outflow plate temperatures during operation. Five gradient thermometers, consisting of paired thermometers at a calibrated separation to indicate temperature gradients, were installed on the heater glass and aluminium surfaces.

These observations were used to calculate heater losses and to calibrate the heat exchange model to point observations of temperature gain, usually at or near the daily solar peak. These point observations were carried out intermittently rather than daily, with randomisation of air flow rates to calibrate the model for varying flow.

Insolation Measurements

The measurement of direct solar radiation in units of power intensity, W/m^2, is a significant challenge. Readily available commercial light meters are designed to measure illumination rather than solar power. The conversion from luminance measurements (lux, or lumens/m^2) to power (W/m^2) is uncertain because of the variable energy-effectiveness of sunlight.

The instrumented solar panel is in effect a bulk pyranometer. Surface temperature gradients correspond to radiation and conduction losses, while mass inflow-outflow temperatures correspond to heat output. The sum of these power outputs and losses must correspond to solar power, the only thermal input.

The bulk theoretical model back-calculates solar power as a calibration parameter for the temperature data, assuming thermal parameters of emissivity, absorptivity and heat exchange. The resulting "measured" values of solar power are in the range of 600 – 900 W/m^2 during periods of sun, more difficult to measure in low sun.

The upper range seems high, since the solar constant or top-of-atmosphere insolation of 1370 W/m^2 is reduced to around 50% by atmosphere, which should give a maximum of around 800 W/m^2. Armidale's altitude of 1070 m may produce relatively small atmospheric interference effects and a uniquely economic solar budget.

To resolve this question with recognised data, a commonly reported Winter insolation onto a horizontal surface in Armidale is around 8 to 13 MJ/m^{2}day (June interquartile range 8.4 – 12.8) (Solar Armidale Project[3], 2001; Maklad[4], 2014). Continuous temperature records obtained in the course of this project tend to agree with that range: average heat output per day for the 1.82 m^2 panel is 6 kWh/day, corresponding to 11.9 MJ/m^{2}day, which is close to the expected value of daily solar radiation data for this period.

The panel's solar orientation must increase solar performance compared to a horizontal surface, but the exchanger operates at less than 100% efficiency. These two effects may nearly cancel, suggesting that the heater is capable of effective thermal output similar to net solar input for an equivalent horizontal surface at this altitude. The agreement of measured performance data with local insolation data supports this useful rule-of-thumb.

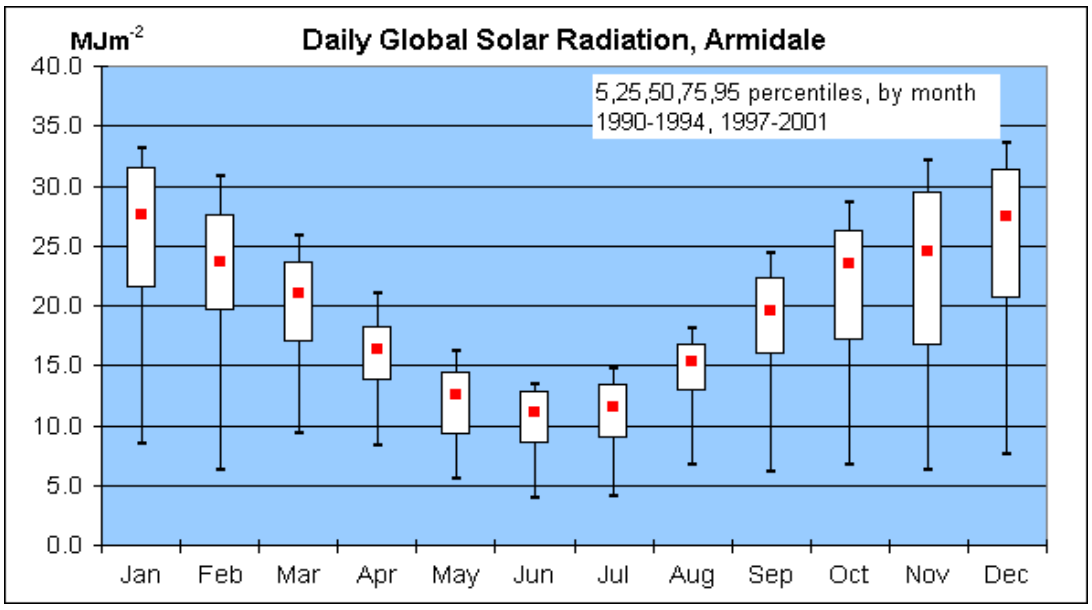

Figure 10: Solar Radiation Data for Armidale. http://www.3sc.net/solarm/solrad2.htm

See also Maklad, 2014. Mean daily heater output in May-June observation is **10.3 MJm^{-2}**

[3] www.3sc.net/solarm/solrad2.htm

[4] Maklad, Y. 2014. *Generation of an Annual Typical Meteorological Solar Radiation for Armidale NSW Australia.* IOSR Journal of Engineering, ISSN (e):2250-3021, ISSN (p): 2278-8719 Vol. 04, Issue 04 (April 2014), |VI| pp 41-45

Airflow Measurements

The difficulty of low-pressure duct air flow measurements was addressed by new purchase of calibrated environmental multimeter hardware. The calibration certificate of the hardware was checked and corrected by direct measurement of laboratory airspeeds. Corrections were obtained by regression of airspeeds measured directly and by anemometer.

Outflow duct air speeds were then measured by the calibrated anemometer on a circular grid of 21 measurement points on the outflow duct, including a near-boundary layer 16 mm from the duct wall. Area-average airspeeds were calculated and applied as $q = vA$, then summed to give the warm air flow rate at protocol speeds between 40% and 100% of pump capacity. The velocity profile was checked against a Prandtl $1/7^{th}$ power-law model.

Outflow temperature and barometric air pressure measurements were combined to calculate warm air density using the ideal gas density law: $\rho = P/RT$ where R = 286.9 J/kgK. Pressure and temperature measurements are used in absolute values.

Density and volumetric flow rate measurements were then combined to calculate mass flow rates at protocol levels:

$$\dot{m} = \rho.q \qquad \text{(Mass flow rate, kg/s)}$$

Mass flow rate is constant in a given steady state at all points in the air flow. This correlates the heater output to the temperature gain:

$$\dot{Q} = \dot{m} C_p \Delta T \qquad \text{(Heat flow rate, Watts)} \qquad (2)$$

The dotted terms indicate constant flow rates of heat ($\dot{Q}$) and air mass ($\dot{m}$).

Heater Power and Efficiency Calculations

There is a competing balance between the temperature gain and the thermal power of the heater, with an optimum point that may coincide with optimum thermal efficiency, depending on a number of factors including the development of the turbulent heat transfer coefficient.

Efficiencies of the heating process are calculated by comparison to total insolation, and also by comparison to total heat absorption plus fan power input. These two efficiencies, referred to as solar efficiency and input efficiency, are independent estimates of heater performance compared to ideal and real conditions.

Solar efficiency is defined as the net heater output compared to net insolation over the external plate surface area regardless of incidence cosine or absorptivity. This is to compare the heater's operation to an ideal solar element such as a direct-incidence non-reflective skylight of the same area. This ideal efficiency is a reference minimum rather than a realistic target, since absorption, reflection and incidence cosine are unavoidable loss factors.

Input efficiency compares the heater's output to the sum of absorbed solar power and fan electrical power inputs. This measures the heater's losses due to re-radiation, conduction and convection at the operating temperatures, relative to physically achievable absorption and incidence factors, and includes the operating cost of the fan.

Since the external heat loss modes (radiation, conduction and convection) all increase with temperature it can be expected that input efficiency will increase with flowrate, as temperatures in the plate and glass/aluminium surfaces decrease with flowrate.

Flow rate control is limited by sunlight and by the increasing electrical cost of the fan, which cannot extract more heat than is available from the limited solar input. Solar efficiency at peak input efficiency indicates the maximum effective solar power that the unit can extract.

It is also useful to calculate a power amplification factor, defined as the ratio of heater thermal output to electrical input due to the operation of the fan. Since fan power varies between 10 and 80 watts, while heater output varies between 400 and 1200 watts, the amplification factor can be anywhere between 5x and 120x, that is for every 1 kWh of electrical energy input, between 5 and 120 kWh of heat are produced.

The amplification factor reflects a net energy gain obtained from the sun, the basic rationale for this type of solar heating. Finding optimum amplification factors that do not compromise total heat output and efficiency is a goal of this research.

Fan power consumption varies as the square of flowrate, with a nominal electrical efficiency of around 70%. A simple model of this for an 80 Watt, 140 l/s fan at 1000 m would be:

$$Q_{fan} = 80\frac{\dot{m}^2}{0.147^2} = 3700\dot{m}^2 \qquad \text{fan electrical power (Watt)} \qquad (9)$$

The efficiency factor of 0.7 is not shown here as the fan's nominal electrical power of 80 W includes that value in relation to the production of peak mass flowrate at 0.147 kg/s.

The three forms of efficiency are calculated as:

$$\xi_{solar} = \frac{\dot{Q}}{insolation} = \frac{\dot{m}C_p\Delta T}{IA_e} = a\cos(\alpha) - 1.05\frac{e\sigma}{I}\left(\text{average}\left(T_{plate}^4\right) - T_{ambient}^4\right)$$

$$\xi_{input} = \frac{\dot{Q}}{absorption + Q_{fan}} = \frac{\dot{m}C_p\Delta T}{aIA_e\cos(\alpha) + 3700\dot{m}^2}$$

$$\xi_{amp} = \frac{\dot{Q}}{Q_{fan}} = \frac{C_p\Delta T}{3700\dot{m}}$$

This set of comparisons is complex and depends on the actual effectiveness of the system to increase building temperatures over a range of flow rates and climate conditions. The target is to jointly optimise all three forms of efficiency, as well as to locate the optimum thermal power output by flow rate in relation to optimum building temperatures.

Heater Power: Thermodynamic Analysis

The heater's thermal power is measured by combining the mass flow rate and air temperature gain with the specific heat capacity of air. This value, C_p = 1005 J/kgK, is the amount of heat energy required to raise a 1 kg mass of air (typically 1 m^3 at 1000 m altitude) by 1°C:

$$Q = mC_p\Delta T \qquad \text{(Mass heating, Joules)} \tag{1}$$

The heated mass m is in steady state flow through the heating system, hence the heat energy flow rate is related to the mass flow rate in steady state:

$$\dot{Q} = \dot{m}C_p\Delta T \qquad \text{(Heat flow rate, Watts)} \tag{2}$$

ΔT is the temperature gain in the air flow. This depends on the heat exchange process, which is driven by the plate-air temperature difference and by the time spent in the heat exchanger. Both of these factors can be increased by reducing the flow rate.

Heat exchange is parameterised by a heat transfer coefficient h:

$$\dot{Q} = h.A_t\left(T_{plate} - T_{air}\right) \tag{3}$$

where A_t is the transfer area of the plate, designed as a large multiple of the external surface area. The heat transfer coefficient h is maximised by ensuring turbulent flow through the exchanger. The effect can be estimated by laminar-turbulent correlations such as Hausen-Seider-Tate and varied by trial and error as a calibration process to match experimental data.

Since the plate-air temperature difference is constant for a given steady state, the temperature gain in airflow through the heater is a linear relationship between equations (2) and (3):

$$\dot{m}C_p\Delta T = h.A_t\left(T_{plate} - T_{air}\right)$$

or
$$\Delta T = \frac{hA_t}{\dot{m}C_p}\left(T_{plate} - T_{air}\right) \tag{4}$$

This combines relevant design dimensions, thermal parameters, operating conditions and the observed constant temperature difference between the heating plate and heated airflow. The warm air mass flow rate can be estimated by outflow airspeed, temperature and pressure:

$$\dot{m} = \frac{P}{RT}vA_{duct} \tag{5}$$

where P and T are absolute pressure and temperature and vA_{duct} is the velocity-area continuity or volume flowrate, measured at the warm air outlet.

It can be seen that the temperature gain ΔT increases in direct proportion to the heat exchange parameter hA_t but in inverse proportion to the mass flow rate. There is a need to determine optimum flow conditions for installation variables such as house volume and heat loss rate, as well as local climate variables such as seasonal insolation and ambient temperatures. Householder preferences are also involved in the selection of an output temperature.

Thermal Inputs and Losses

The temperature difference between heating plate and internal airflow is obtained by considering the rates of heat loss and heat exchange as functions of plate temperature.

The internal heat exchange process consists of mixed convective, conductive and radiative effects (in decreasing order of effect size), while external losses are predominantly radiative through the Stefan-Boltzmann process on the heated plate. There are also relatively minor conductive and convective losses from glass and aluminium surfaces of the heater box. The 2015 pilot study indicated conductive and convective losses approximately 5% of radiative losses in still air, with up to twice that amount in strong wind.

In steady state the internal heat transfer rate must equal the net insolation minus losses:

$$\dot{Q} = h.A_t\left(T_{plate} - T_{air}\right) = A_e\left(aI\cos(\alpha) - 1.05e\sigma\left(\text{average}\left(T_{plate}^4\right) - T_{ambient}^4\right)\right) \qquad (6)$$

where A_e is the external (emission) surface area, aI is solar heat absorption based on local insolation I and the surface coating's rated absorptivity a. The cosine of the plate's orientation relative to solar altitude and azimuth is also applied. The factor of 1.05 estimates the effect of conductive heat loss, increasing to 1.1 to allow for convective loss in strong wind. External surfaces remain cool during operation, so these losses are almost negligible.

The emission coefficient e is optimised to minimise heat loss by selection of a low emission commercial solar coating on the external surface. The coating product's rated emissivity of e = 0.35 and absorptivity a = 0.9 are used in these calculations. Emission and absorption are not equal as heat is extracted by the internal airflow, hence it is reasonable to allow this large difference in absorption-emission even in the system's steady state operation.

The Stefan-Boltzmann constant σ = 5.67x10^{-8} W/m^{2}K^4 parameterises the emission process. Fourth-power average plate temperature T_p^4 and ambient temperature T_a^4 are standard in radiative theory. The constant temperature gradient enables a definite integral of the fourth-power average plate temperature T_p^4 to a fifth-order polynomial. This is closely approximated by a simple 4th power average.

The observed constant plate-air temperature difference can thus be calculated on the basis of design variables and local insolation measurements:

$$\left(T_{plate} - T_{air}\right) = \frac{A_e}{hA_t}\left(aI\cos(\alpha) - 1.05e\sigma\left(\text{average}\left(T_{plate}^4\right) - T_{ambient}^4\right)\right) \qquad (7)$$

This is used to calculate the temperature gain:

$$\Delta T = \frac{hA_t}{\dot{m}C_p}\left(T_{plate} - T_{air}\right) = \frac{A_e}{\dot{m}C_p}\left(aI\cos(\alpha) - 1.05e\sigma\left(\text{average}\left(T_{plate}^4\right) - T_{ambient}^4\right)\right) \qquad (8)$$

Heat exchange can thus be attributed to net insolation aIA_e.cos(α) reduced by external heat losses, while temperature gain is inversely proportional to mass flow rate.

Note the inverse (cooling) effects of hA_t in (7) and $\dot{m}$ in (8). Increasing either of these factors produces cooler plate temperatures and lower radiative losses. This offers a choice between

increased heat flow and higher efficiencies at high flowrates, or increased temperature gain with lower efficiency at low flowrates.

It can be seen that at very high flow rates the temperature gain is small, limiting the effectiveness of heating despite extracting a large proportion of the available solar power. Conversely at very low flow rates the temperature gain is large but may fail to circulate through a building, with negligible effective heating.

Numerical Modelling and Experimental Calibration

The theoretical model consists of linked implicit formulae (7) and (8) that must be solved by iterative methods. The plate temperature depends upon itself and is correct only when T_{plate} values on both left and right sides of the equation are numerically equal. This was done using a spreadsheet with iterative calculations. The output is corrected in each calculation step until the solution converges on predicted plate temperatures and outflow air temperature.

The model was calibrated to experimental data on plate temperatures and inflow-outflow air air flow rates and temperatures, following an experimental protocol whereby the warm air flow rate was varied from day to day by small steps between 40% and 100% of peak flow rate. Continuous building temperatures were also recorded and correlated to the flow regime and ambient temperature on those days. Once-weekly "off" days were allowed in the protocol, as these show the building's thermal behaviour in the absence of heating.

The model applies the protocol flow rates and measured temperatures by numerically optimising the theoretical fit to data. The two key calibration variables are the net radiative absorption into the heating plate and the turbulent heat transfer coefficient. This solves for the temperature gain, with small errors in the plate temperature indicating the size of error in the estimated temperature gain.

Model heat transfer coefficient and insolation are varied by trial-error until the observed temperature gain and plate-air temperature difference are predicted within 1^{o}C. This is repeated for each protocol flow rate and the fit to parameters improved by multiple repetitions over the course of the winter months.

Turbulent Heat Transfer Coefficient

A key optimisation objective in the original design process for the heat exchanger was to maximise turbulence in the flow through the exchanger channels. Turbulence increases fluid mixing, in particular the mixing of hot boundary layers with cooler inflowing air. Optimum heat transfer coefficients can be found by designing channel dimensions and flow velocities to produce large a Reynolds number, the key indicator of turbulence:

$$\mathrm{Re} = \frac{vD_h\rho}{\mu}$$

where D_h is the hydraulic diameter of the channel and μ is the viscosity of the airflow, around 1.85×10^{-5} Pa.s at operating temperatures. Reynolds values greater than 2000 begin to develop turbulence, which transitions from flow instabilities to eddies and vortices as Reynolds number increases from 4000 to around 10,000. Above this value, turbulence continues to develop and to a lesser degree improves the heat exchange characteristics of air flow.

A compromise must be found between a large heat transfer area consisting of multiple closely-spaced fins and the small hydraulic diameter of a narrow channel between fins. The flow velocity is relatively insensitive to fin spacing, increasing by a factor of only 2 between a flat internal plate and a "comb" design where fins occupy half the available area. The hydraulic diameter however decreases by a factor of 29 over the same design range, so a closer fin design always produces a smaller Reynolds number for a given flow rate: The Reynolds number decreases by a factor of 2/29 or nearly 1/15 over the design range.

The transfer area A_t increases with fin density, by a factor of 27 over the same range, suggesting that the transfer area may significantly dominate the combined design parameter hA_t in this range. Assuming the worst case of a linear proportional decrease in h with decreasing Reynolds number, the design parameter hA_t would tend to increase monotonically with fin density, by a factor of 27/15 or about double in the design range.

To resolve this question, heat transfer coefficients were calculated theoretically and by back calculation from the operating heater thermal data. Theoretical calculations used the Hausen Correlation for laminar flow (Hausen[5], 1959) transitioning to the Sieder-Tate correlation for turbulent flow (Incropera and DeWitt[6], 2000). These were compared to the experimentally calibrated heat transfer coefficient obtained by iterative trial and error.

Good numerical agreement was found between theoretical and experimental h values. The functional trends of the theoretical and experimental curves are slightly dissimilar however the overall correspondence is an excellent order-of-magnitude estimate given the uncertainties in the data. This is the optimum calibration of the model to temperature data as described above.

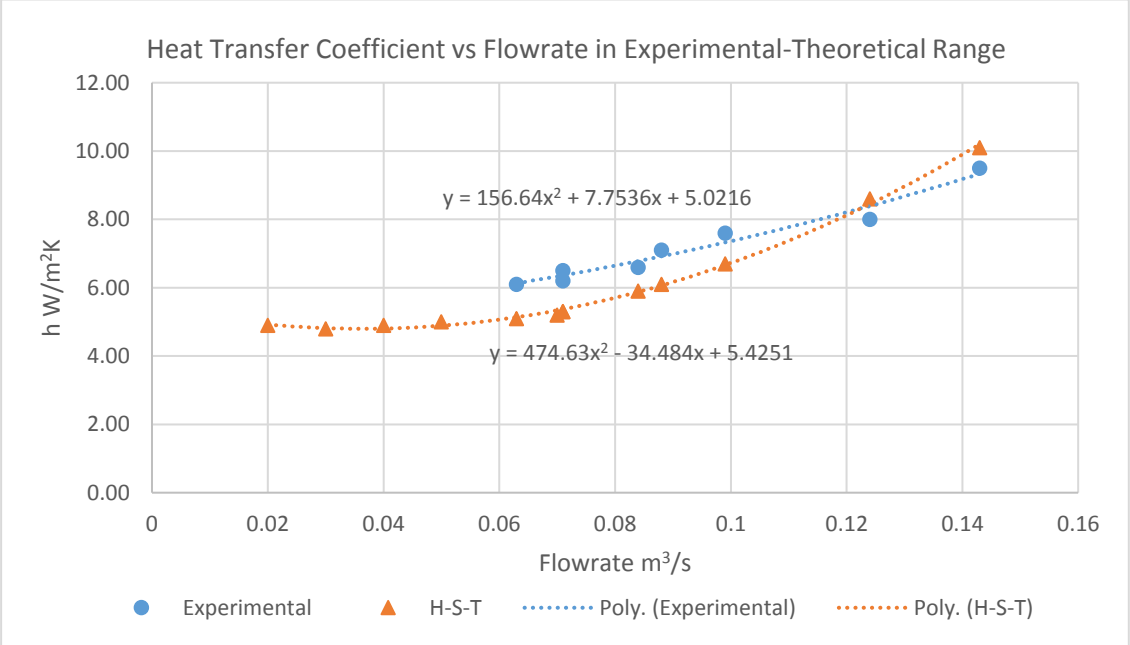

Figure 11: Comparison of Experimental and Theoretical Heat Transfer Coefficient

Both functional trends were analysed. The limitations of experiment on one design over a narrow flow range suggested a suitable level of detail would be a simple linear increase in h with Re,

[5] Hausen, H 1959. Neue Gleichungen fur die Wurmeubertragung bei freier und erzwungener Strmung (New equations for heat exchange in free and forced convection) Wurmetechnik **9**, 75-79

[6] Incropera, FP and DeWitt, DP 2000. *Fundamentals of Heat and Mass Transfer* (4th Edn) Wiley, NY p. 493 ISBN 0-471-30460-3

which led immediately to the foregone conclusion that A_t would dominate the process. This was not regarded as reliable, even if probable.

The theoretical analysis involved calculation of the Prandtl number, a dimensionless number representing the ratio of convective to conductive heat exchange, typically $Pr = 0.7$ for air in the operating temperature range, as well as air viscosities in the main stream air flow and at the plate temperature. The Hausen and Sieder-Tate correlations are inversely proportional to hydraulic radius, with the result that heat transfer coefficient tends to decrease with Reynolds numbers greater than 10,000 for very large fin spacings, but to increase as Reynolds numbers decrease less than 3000 for very small spacings.

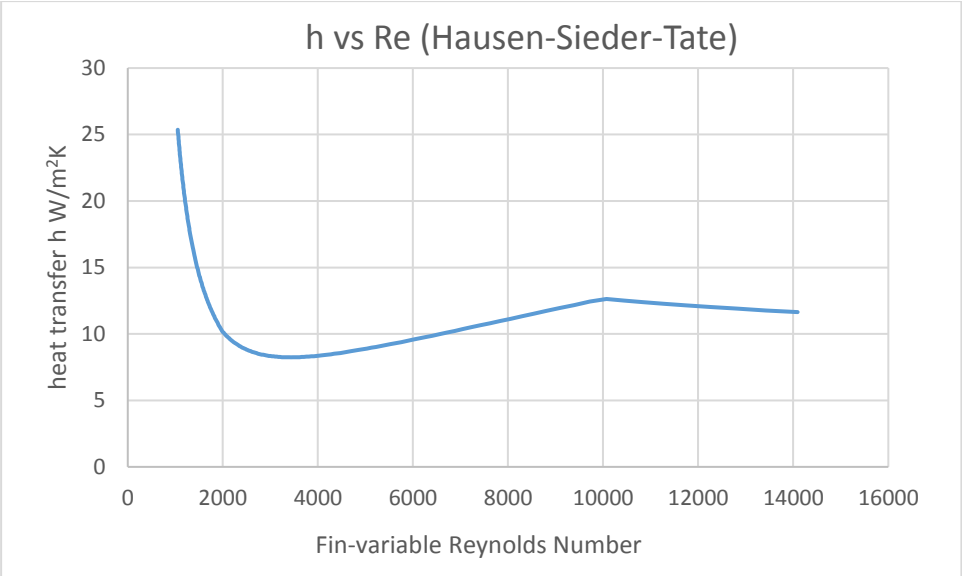

Figure 12: Graph of heat transfer coefficient with design Reynolds number

The expected linear proportionality of heat transfer coefficient with Reynolds number occurred only in the Reynolds 3000-10,000 range, while transfer area increased monotonically with fin density regardless of fluid variables. As a result it was found that the combined design parameter hA_t is dominated by A_t and increases monotonically with increasing fin density, further supported by a radically increasing h in the low Re range driven by small hydraulic diameter.

The experimental heat transfer coefficient is closely approximated by a polynomial correlation to warm air flow rate q in m^3/s:

$$h = 156.64q^2 + 7.7536q + 5.0216$$

This experimental heat transfer coefficient data-model is preferred over the general theoretical model for analysis within the prototype-tested ranges of flow and temperature. In general, using this model, heat output tends to increase with flow rate, countered by decreasing input efficiency and smaller temperature gains as expected from observation.

Thermometric Data and Analysis

Continuous Duct Temperatures

Continuous data on cool / warm duct airflow and external sun-ambient temperatures were collected from 22 May to 1 July. The data from this instrumentation are graphed in Figure 13.

The temperature gain between cool and warm airflow temperatures are correlated with flow rate and solar temperature. Instantaneous heater output is calculated from this data by subtracting warm-cool temperature gain and multiplying by the flowrate. Air heat capacity 1005 J/kgK converts this to heater power in thermal watts. The result is displayed as continuous analysis in Figure 14.

The inverse relationship between air flowrate and temperature gain is apparent. In a first test (Figure 16), flowrate was varied from 143 l/s to 58 l/s then 71 l/s on 23-25 May, with large changes in temperature gain but relatively small inverse changes in heater power. The result on 25th May is regarded as an ideal warm weather temperature gain and high heater output.

The flowrate 70 l/s stands out as an optimum value that provides a balance of high temperature gain and high heater output. This can be improved by local experimentation on an installed system in well-insulated commercial or residential premises.

The system can produce peak heat power of around 1600 W (Figure 19). Low sun periods continue to produce significant heatflows, seldom less than 800 W on average in a day and often as high as 1200 W. It can be seen in the theoretical comparions that this is at a high efficiency, up to 80% direct solar efficency and 90% input efficiency.

These results were surprising in the original design calculations and pilot study but are expected values in the current study. The challenge in installation is to ensure that this good potential for thermal power is suitably design-installed, insulated to retain heat and use-tested for optimum input and flowrate matching to available sunlight.

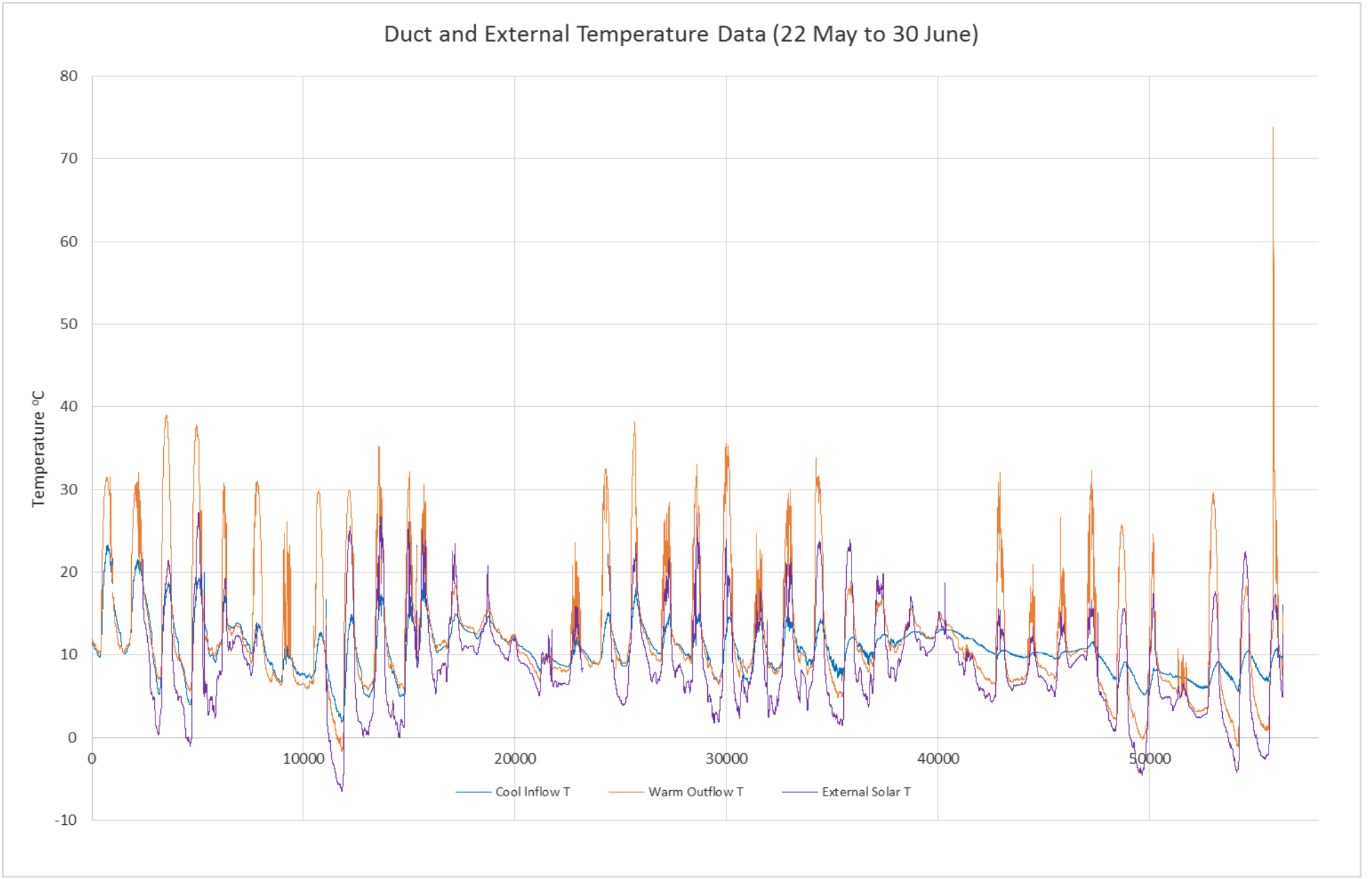

Figure 13: Continuous temperature data in cool and warm duct airflow, and external solar-ambient temperature. Dates are from 22 May to 30 June

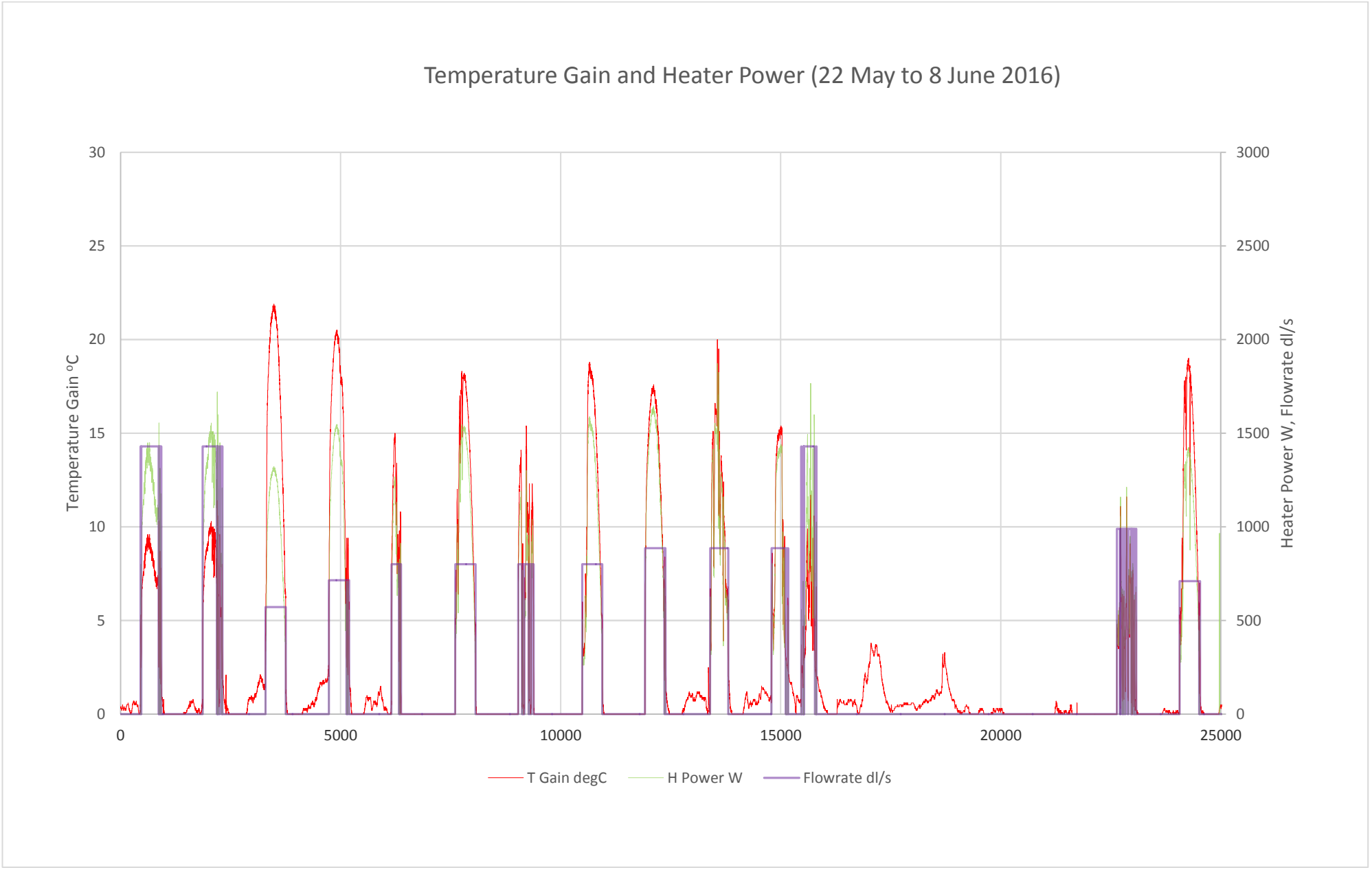

Figure 14: Temperature gain and heater power derived from continuous temperature data in Figure 13 (22 May to 8 June).

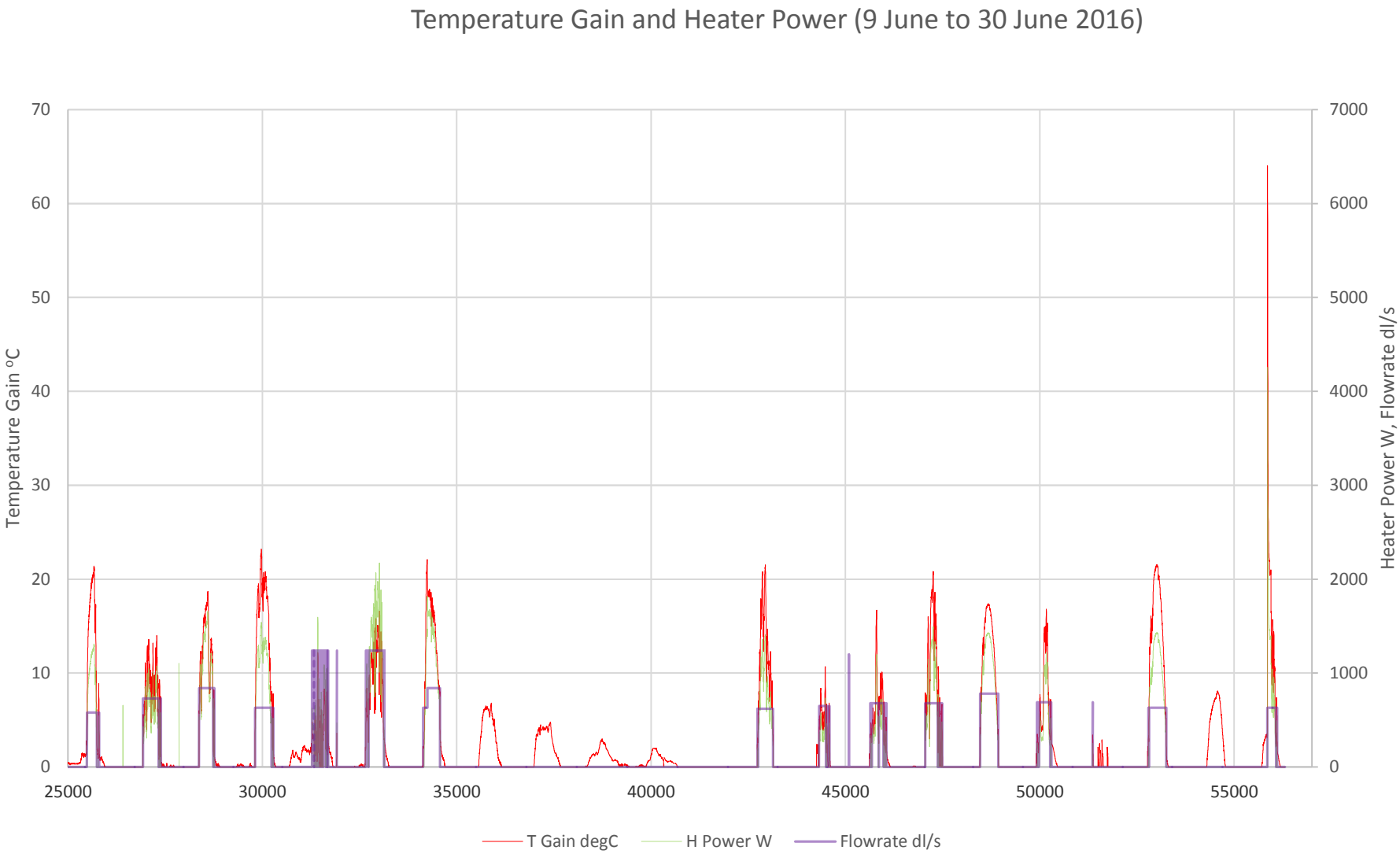

Figure 15: Temperature gain and heater power (9 to 30 June).

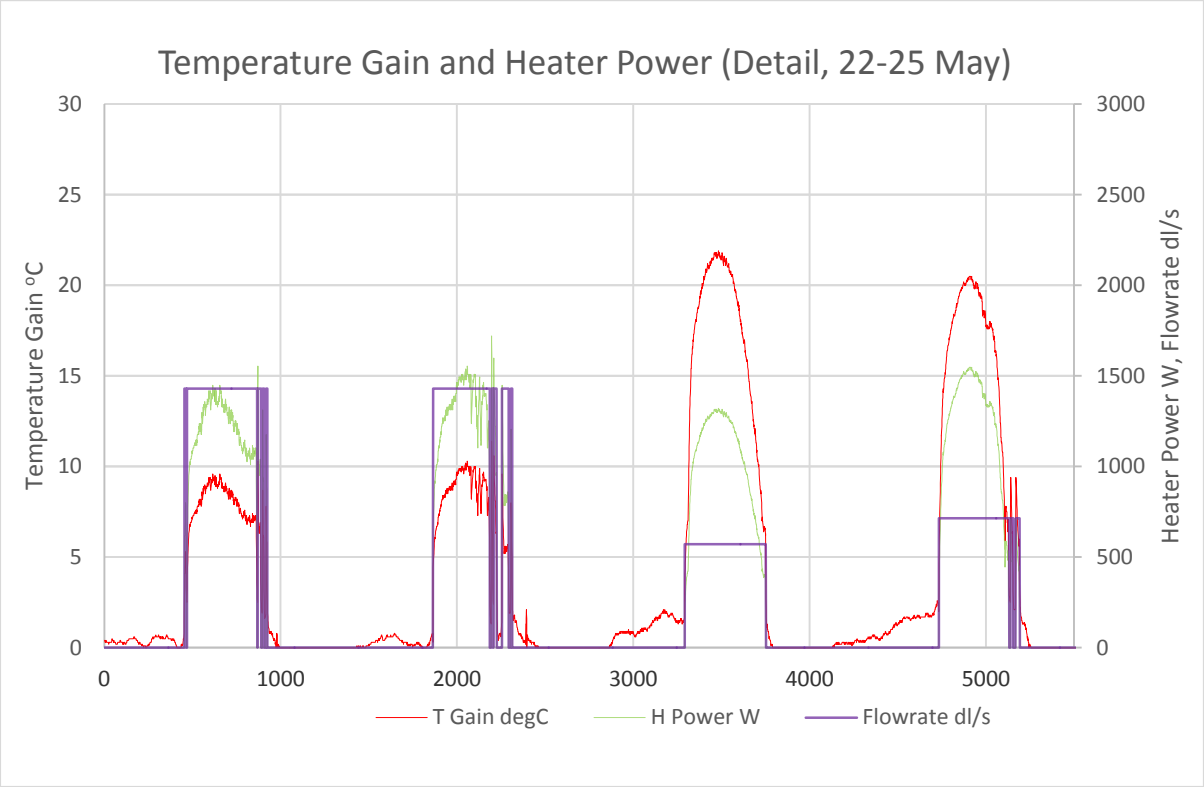

Figure 16: First four days of continuous analysis: 143 l/s flow rate in the first two days proves unreliable in light overcast: this is adjusted to 58 then 71 l/s (days 3 and 4). This produced a dramatic increase in temperature gain, corrected to restore heater power.

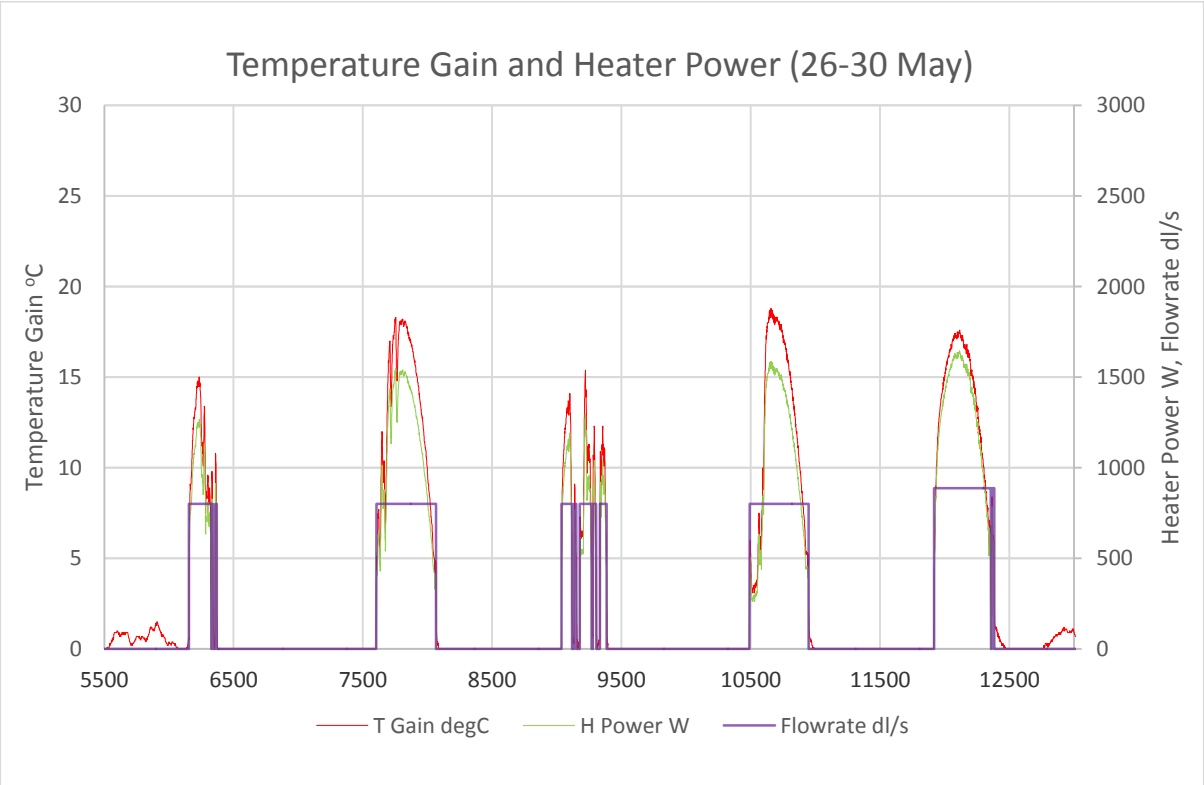

Figure 17: Next five days: trying to get a good run on 80 l/s, then increase to 89 l/s. Again the effect on temperature gain is strongly correlated to flowrate. Heater power is less sensitive to flowrate but is strongly correlated to available sunlight..

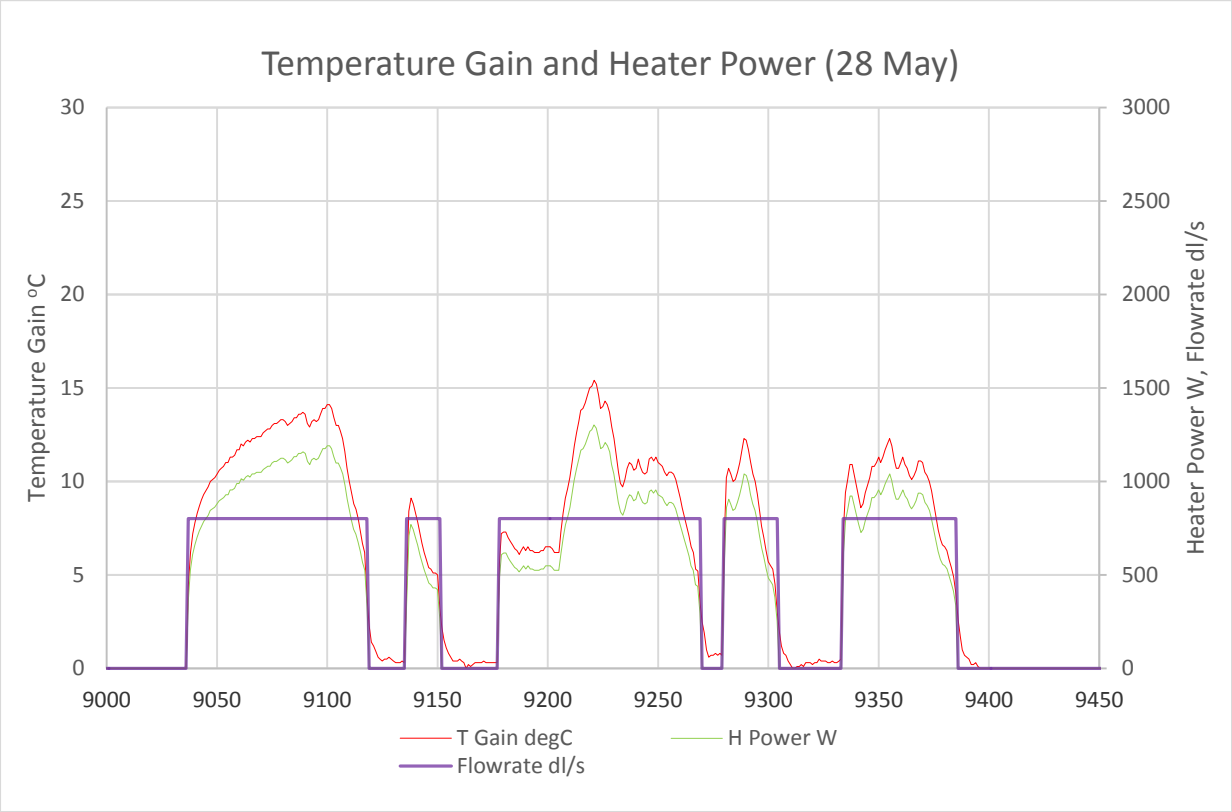

Figure 18: Detail of analysis for 28/5/2016. High flow at 80 l/s and intermittent cloud limited temperature gains and heater power to 10-12°C and 600-1000 W

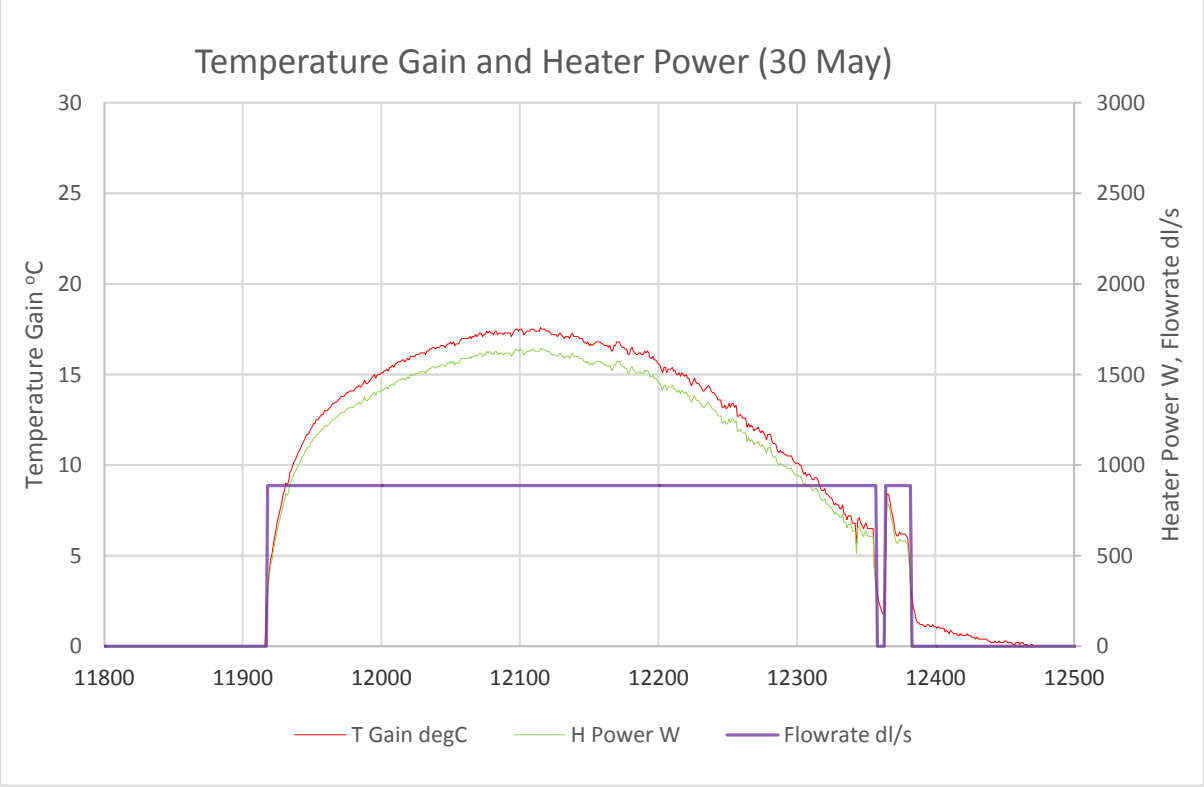

Figure 19: Detail of analysis for 30/5/2016. Warm weather and intermediate flowrate produced a very large heat output with high temperature gain. The flowrate at 89 l/s is not ideal, and could be improved in by local experimentation. Operates 8:44am to 4:29pm.

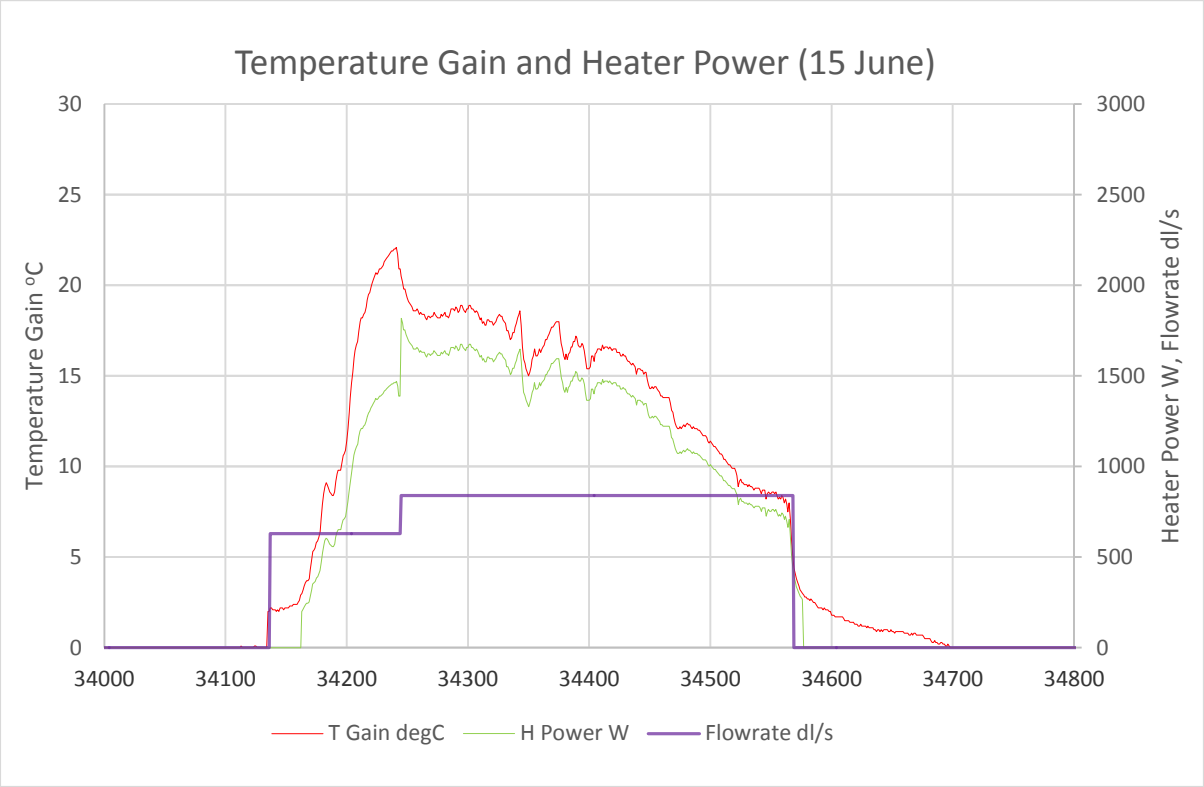

Figure 20: Detail of analysis for 15/6/2016. Early fog suggested a low flowrate, 63 l/s. Emerging sun suggested an 11am increase, to 84 l/s. The tendency to overgain the temperature at low flow in high sun is corrected and heater power increased, with a small prime blowoff. Operates 9:12am to 4:24pm

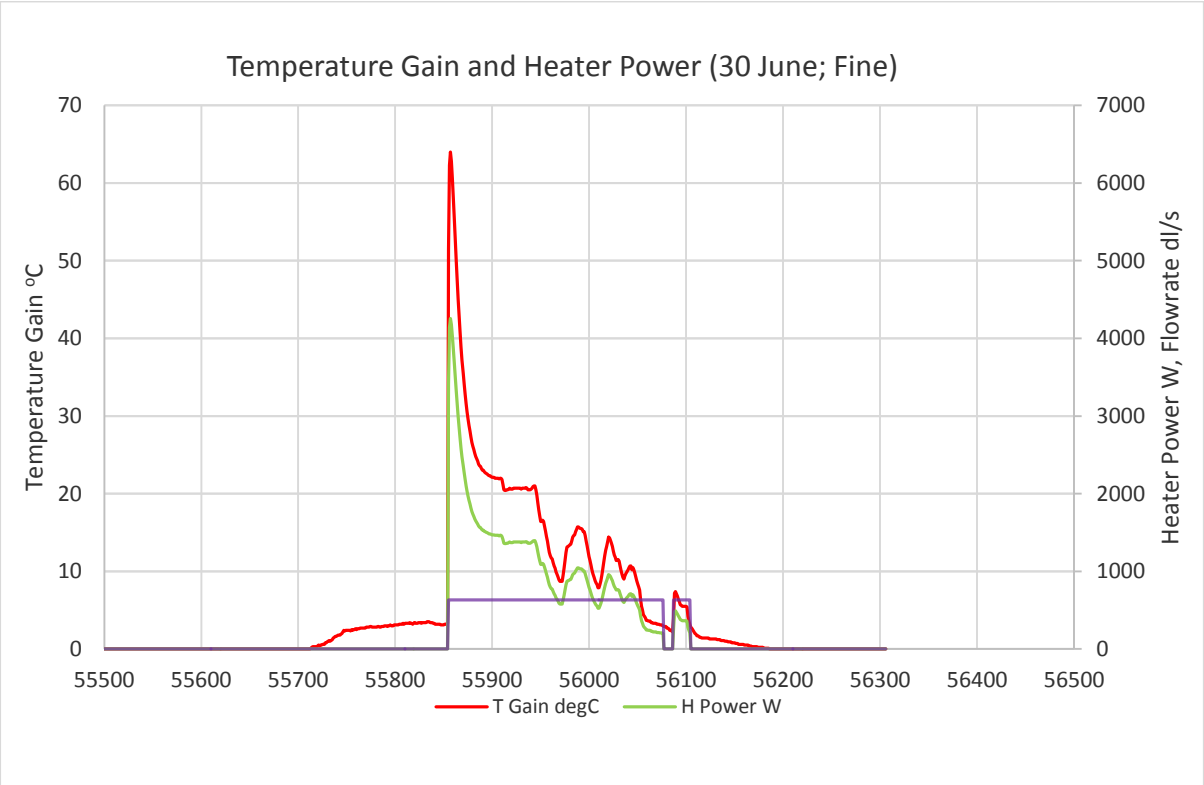

Figure 21: Detail of analysis for 30/6/2016. Heater off in in full sun to prime until 11:55, then on at 63 l/s. Peak temperature gain & power were 65 degrees at 4200 W. Output decreased to 22°C at 1400 W over oner hour. This released 2.2 kWh in one hour, 4.4 kWh for the day. In volume-temperature terms, 226 m^3 were heated in one hour to a mixture temperature of 39°C.

Maximum – Minimum Temperatures

Data on maximum/minimum building temperatures were collected daily from 17 May to 1 July. The data from this instrumentation are graphed in Figure 22.

Graph Acronyms:

S: South
Sw: Southwest
N: North
C: Central at 2 m height
R: Ceiling at 4 m height, above C
Tc: Cool intake
Tw: Warm outlet
o: Outside
i: Inside
x: Maximum
m: Minimum
ie Swix: Southwest inside maximum

The 4 m ceiling and 2 m head height positions represent an expected value of temperatures in the working area of the building. It is evident from the graph that these temperatures are generally distinct from other maximum and minimum temperatures, but the relative effect of the heater is not immediately obvious.

The effect of the heater can be examined by comparing data labels, the label "Off" indicating that the heater is off. Weather conditions are also indicated by label. It is evident that the maximum temperatures at ceiling and centre positions become less distinct in off periods. This can be tested statistically by grouping temperature differences for on and off states and analysing them as independent variables.

There is a significant difference ($p = 7E-7$) at ceiling level and at 2m height ($p = 0.009$) between the compared maximum temperatures. The elevation of maximum ceiling-level temperature can be attributed to the effect of the heater. The actual temperature difference is small but detectable and agrees with comments from workers in the shed that the heater provides a noticable improvement in the warmth of the building.

Comparison of the labelled weather conditions suggests that the heating effect is most noticeable in periods of light overcast. The shed is warmed to a substantial degree by direct sun on the northern wall, which obscures the effect of the heater in those periods. Very low-sol conditions do not produce significant heater power when building temperatures are most reduced. In intermediate conditions the effect of the heater is most distinct from the effect of the northern wall.

The warm outflow duct is consistently the warmest maximum temperature in the data, typically $8^{o}C$ warmer than the northern sun-exposed windows and outside sunny bay. Warm air is distributed in the building, as seen by the significant effect attributed to the heater.

This analysis supports the hypothesis of effective heating due to the solar heater in periods of sun and light overcast. In an insulated building the effect of direct sun on the building in high-sol weather will be less noticeable and the heater's role would be more evident. This can be tested in a commercial or domestic installation, to follow this second pilot study.

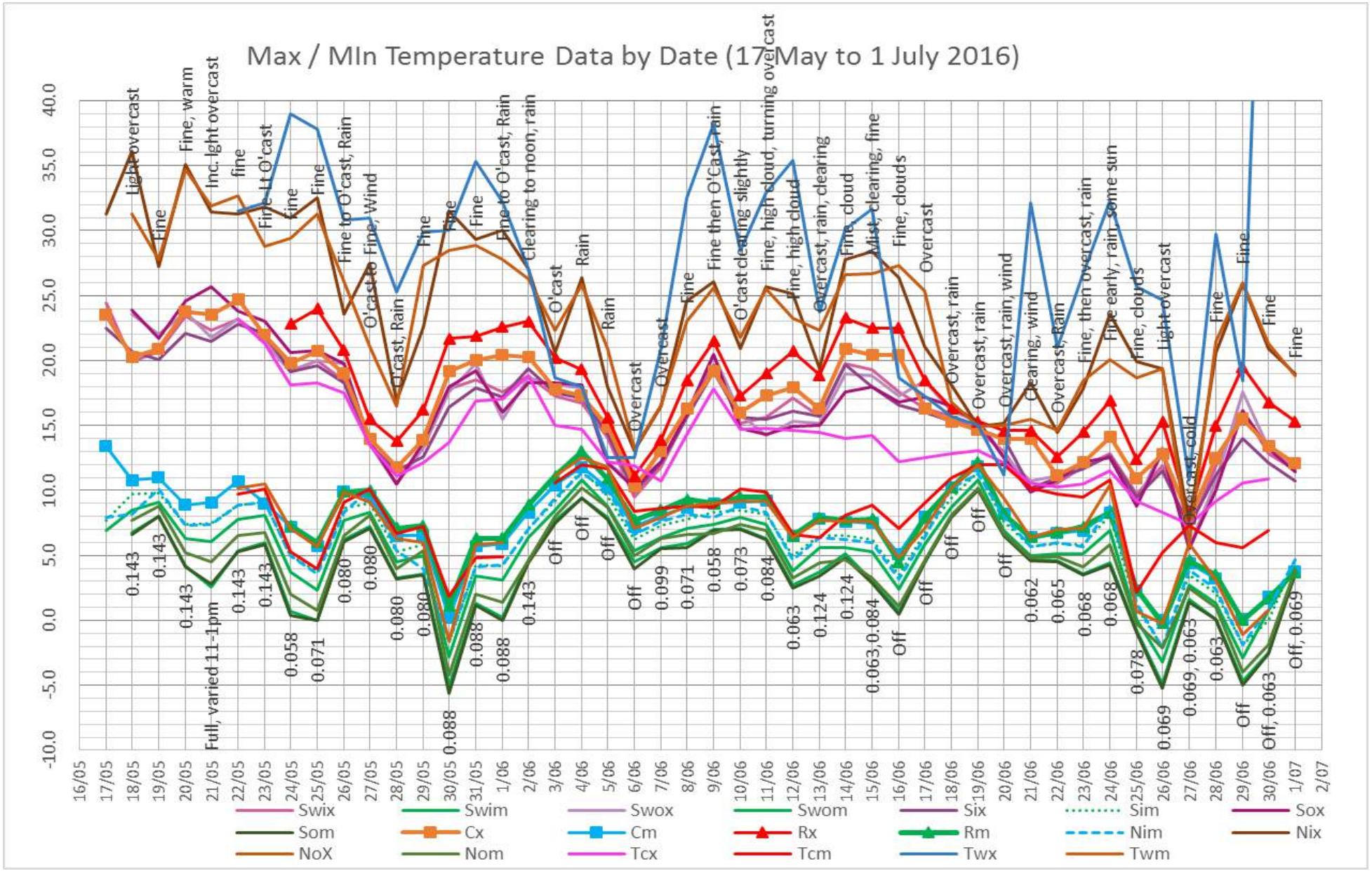

Figure 22: Graph of max/min building temperatures by date. The centre and ceiling positions are visually distinct from north and south walls.

Typical calculation applying thermodynamic theory to thermometric data:

The following calculation uses the 7 June 12:29 pm data to correlate heat output with temperatures for the higher solar level. This resolves within +/- 1.3ºC because of the non-linearity of rapid heating, but gives a balanced estimate of mean plate temperature and an exact estimate of temperature gain as measured.

7 June 2016 12:29pm

Insolation = 800 W/m^2 parameterised
Ambient Temperature = 13.3ºC = 286.5 K
Reduced Air Pressure 1003 hPa
Wind Strong
Inflow Temperature 12.0ºC
Outflow Temperature 23.7 ºC
Inflow Plate Temperature 26.3 ºC = 299.5 K
Outflow Plate Temperature 35.7 ºC = 308.9 K

Warm Flow Rate 0.099 m^3/s
On this atmospheric data the warm air density is 1.05 kg/m^3, $m.$ = 0.104 kg/s
Data + Reynolds and Prandtl numbers give a heat transfer coefficient of h = 7.6 W/m^{2}K
The transfer area (patent information) gives hA_t = 93.4 W/K, C_p = 1005 J/kgK

Insolation absorption into the area-oriented heating plate:

$$Iplt = a.I.cos(\alpha).A_e$$

$$= 0.9 \times 800 \times 0.99 \times 1.815 = \mathbf{1294\ W}$$

Radiative, Conductive and Convective Losses:

$$Loss = 1.1e\sigma A_e(\text{average}(T_p)^4 - T_a^4)$$

$$= 1.1 \times 0.35 \times 5.67\times10^{-8} \times 1.815 \times ((308.9^4+299.5^4)/2 - 286.5^4) = \mathbf{73\ W}$$

Air warming as formulated:

$$T_{warm} = T_{cool} + (aI - 1.05e\sigma(\text{average}(T_p^4) - T_a^4)).(A_e/m.C_p)$$

$$= 12.0 + (1294 - 73) / (0.104 \times 1005)$$

$$= \mathbf{23.7ºC} \text{ as measured.}$$

This calculation converges to within +/- 1.3ºC of the correct plate temperatures:

$$T_{plate} = T_{air} + (Isol - Loss)/hA_t$$

$$= (12.0, 23.7) + (1294 - 73) / 93.4$$

$$= (\mathbf{25.1,\ 36.8})\ ºC \text{ compared to } (26.3, 35.7)\ ºC \text{ actual.}$$

The errors are due to non-linearities as the rapidly warming system is not in steady state.

Heater Power $\dot{Q} = \dot{m} C_p \Delta T$ = 0.104 x 1005 x (23.7 – 12.0) = **1220 W** = 1290 - 70

Input efficiency = $\frac{\dot{Q}}{aI\cos(\alpha)A_e + Q_f} = \frac{1220}{0.9 \times 800 \times 0.99 \times 1.815 + 3700 \times 0.104^2}$ **= 91.5%**

The main uncertainty in this calculation is the flowrate. Considerable effort was devoted to calibrating the anemometer and multi-point measurement of the outflow duct. The full calculation puts the figure in context for this typical case.

Insolation	**Isol**	**W/m^2**	**800**		
Heat Transfer Coefficient	**htrn**	**W/m^{2}K**	**7.6**		
Solar Altitude	Asol	^{o}alt	36.5	36.05^o Solstice	
Solar Azimuth	Zsol	^{o}azi	2.5	0.0^o Noon ~12.5^o/hr	
Reduced Air Pressure	**Pred**	**hPa**	**1004.9**		
Atmospheric Pressure	Patm	Pa	89132	1000	m alt.
Ambient Temperature	**Tamb**	**^{o}C**	**13.3**	286.45	K
Wind	**Wind**	**desc**	**Strong**		
Specific Heat Capacity of Air	Cprs	W/kgK	1005		
Specific Gas Constant of Air	Rair	m^2/s^{2}K	287		
Stefan-Boltzmann Constant	sigm		5.67E-08		
Warm Air Flowrate	**Qwrm**	**m^3/s**	**0.099**		
Mass Flow Rate	Mflr	kg/s	0.104		
Fan Power	Fpow	W	38		
Orientation Cosine	Ocos		0.988		
Area-Cosine Absorption into Plate	Iplt	W	1291		
Plate Temperature Gradient	Kplt	K/m	5.9		
Re-radiation from Plate	Rerd	W	66		
Conduction and Estimated Convection	Clos	W	6.6		
Cool Inflow Temperature	**Tcld**	**^{o}C**	**12**		
Warm Outflow Temperature	**Twrm**	**^{o}C**	**23.7**		
Predicted/Actual Temperature Gain	**DT**	**^{o}C**	**11.7**		
Inflow Plate Temperature	**Tpin**	**^{o}C**	**25.1**		
Outflow Plate Temperature	**Tput**	**^{o}C**	**36.8**		
Net Heater Output	**Hout**	**W**	**1219**		
Total Power Input	Hinp	W	1330		
Direct Solar Power	Psol	W	1452		
Heater Input Efficiency	**zeta**		**91.7%**		
Heater Solar Efficiency	**seta**		**84.0%**		
Heater Power Amplification	**heta**		**31.7x**		

This calculation often resolves within +/- 0.5^{o}C especially if observed at a daily peak. The heat transfer coefficient is used to locate this solution point by iterating plate temperatures.

Performance Forecast Calculations

The inverse temperature control and sunlight response are analysed by co-varying warm air flow rate and insolation. For a given peak insolation at noon, the theoretical model is operated at a range of flowrates. The resulting temperature gains, heater powers and efficiencies are graphed for visual comparison:

Variable flowrate, constant Isol **800 W/m²**						
Warm flow rate Qwrm m^3/s	0.05	0.07	0.09	0.1	0.12	0.14
Temperature Gain ΔT (°C)	22.2	15.8	12.2	11.0	9.1	7.8
Heater Power Hout (W)	1115	1132	1142	1146	1150	1152
Input efficiency zeta	85.7%	86.4%	86.3%	86.0%	85.2%	84.1%
Solar efficiency seta	76.8%	78.0%	78.7%	78.9%	79.2%	79.4%
Power amplifier heta	109	57	35	28	20	14

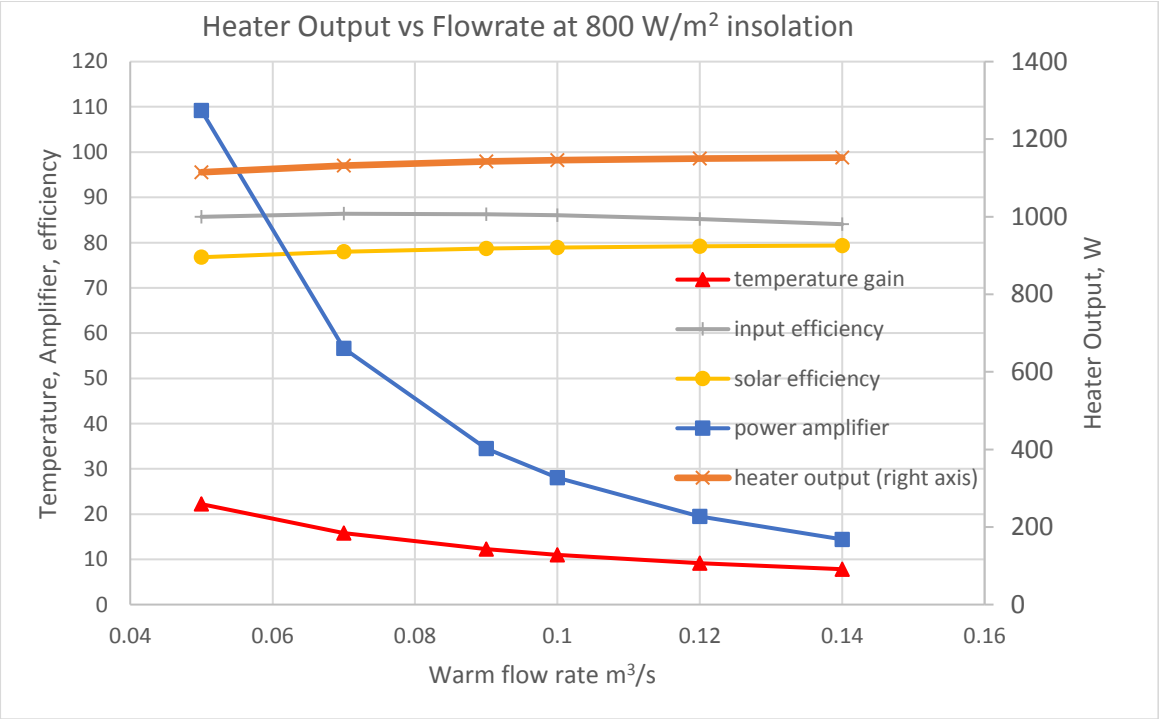

Figure 23: Heater power and temperature gain depend on flowrate, with an optimum around 70 – 80 litres per second

The input efficiency indicates the optimum flowrate for these conditions. The conditions shown are specific to the case specified in this model. Different solar and ambient conditions encountered in practice will effect these numbers. The graph is comparative, indicating optimum flowrate within a 20 l/s range.

The effect of lower solar input is examined by repeating this analysis at a lower solar power, 600 W/m^2. 800 and 600 are selected as typical variations around mean insolation:

Variable flowrate, constant Isol **600 W/m^2**						
Warm flow rate Qwrm m^3/s	0.05	0.07	0.09	0.1	0.12	0.14
Temperature Gain ΔT (^{o}C)	16.3	11.6	9.0	8.1	6.8	5.8
Heater Power Hout (W)	833	845	852	854	857	859
Input efficiency zeta	85.2%	85.5%	85.1%	84.7%	83.5%	81.9%
Solar efficiency seta	76.5%	77.6%	78.2%	78.4%	78.7%	78.8%
Power amplifier heta	82	42	26	21	15	11

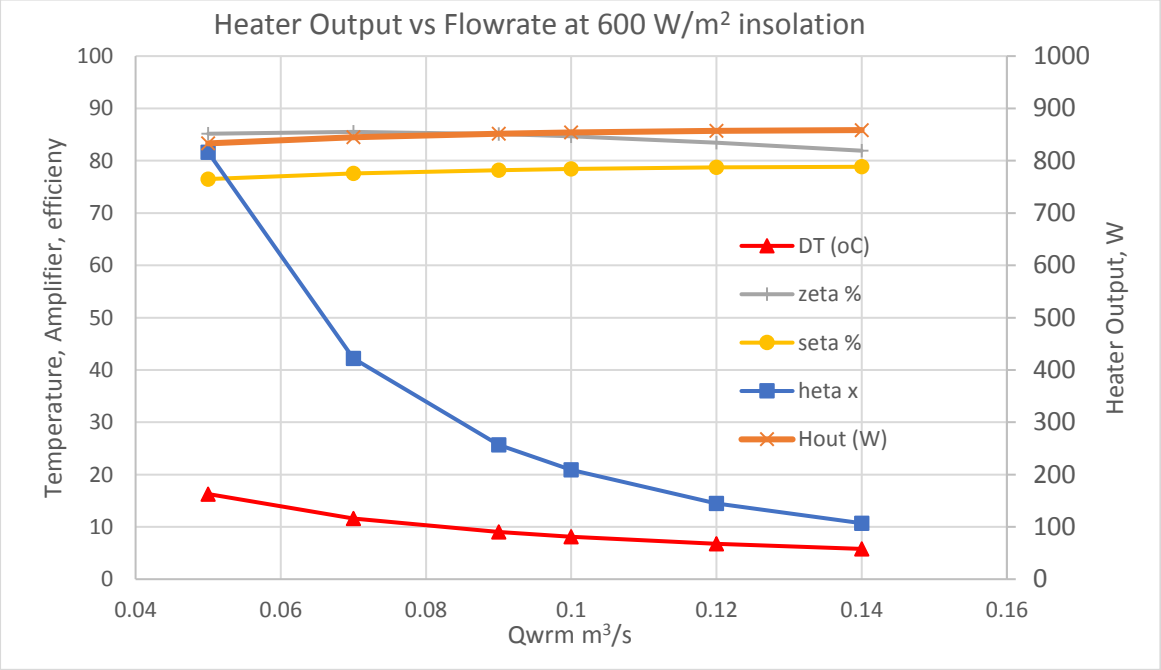

Figure 24: Power and temperature gain are reduced by reducing insolation.

For a 200 W/m^2 reduction in solar input, input efficiency is maintained by reducing the flowrate by about 0.02 m^3/s. This also tends to maintain the temperature gain.

Thermoregulation

A key compromise in the higher heat output of a high flow rate is the reduced temperature gain of the heating effect. Higher flow rates extract more heat from the exchanger and maintain the heating plate at a cooler temperature, resulting in relatively cool air outflow with higher fan power required to drive it. Conversely a lower flow rate increases the temperature of the outflow, but not in proportion; net heat output decreases because the high plate temperature causes higher radiative losses.

Cooler (or warmer) working temperatures at higher (or lower) flow rates operate relative to the heat flow limitations of available solar power in high or low solar conditions; in either case the temperature gain can be controlled by the flow rate. The inverse temperature-heat control suggests that on days of limited solar power the optimal strategy may be to turn the heater down to lower flow rate for warmer temperatures and smaller heat power. The reduced flow would warm a smaller space (eg a kitchen or study area only, excluding bedrooms) at a higher temperature gain, but with reduced power reflecting the reduced solar input.

Flow rate thermoregulation is directly proportional to solar power: for insolation increasing from 200 W/m^2 (heavy overcast) to 900 (extreme full sun), a constant temperature gain can be maintained by increasing air flow rate with solar power. This was modelled theoretically using the polynomial correlation for *h*:

Constant 10ºC ΔT:

Insolation W/m^2	200	300	400	500	600	700	800	900
Warm Flow m^3/s	0.0242	0.038	0.0526	0.067	0.0813	0.0957	0.1099	0.1240
ΔT (ºC)	10.00	10.00	10.00	10.00	10.00	10.00	10.00	10.00
Heater output (W)	253	401	550	700	849	999	1148	1297
Input efficiency zeta	77.7%	81.0%	83.8%	84.8%	85.3%	85.6%	85.9%	85.6%
Solar efficiency seta	69.6%	73.6%	75.8%	77.1%	78.0%	78.6%	79.1%	79.4%
Fan amplifier heta	106x	68x	49x	38x	32x	27x	23x	21x

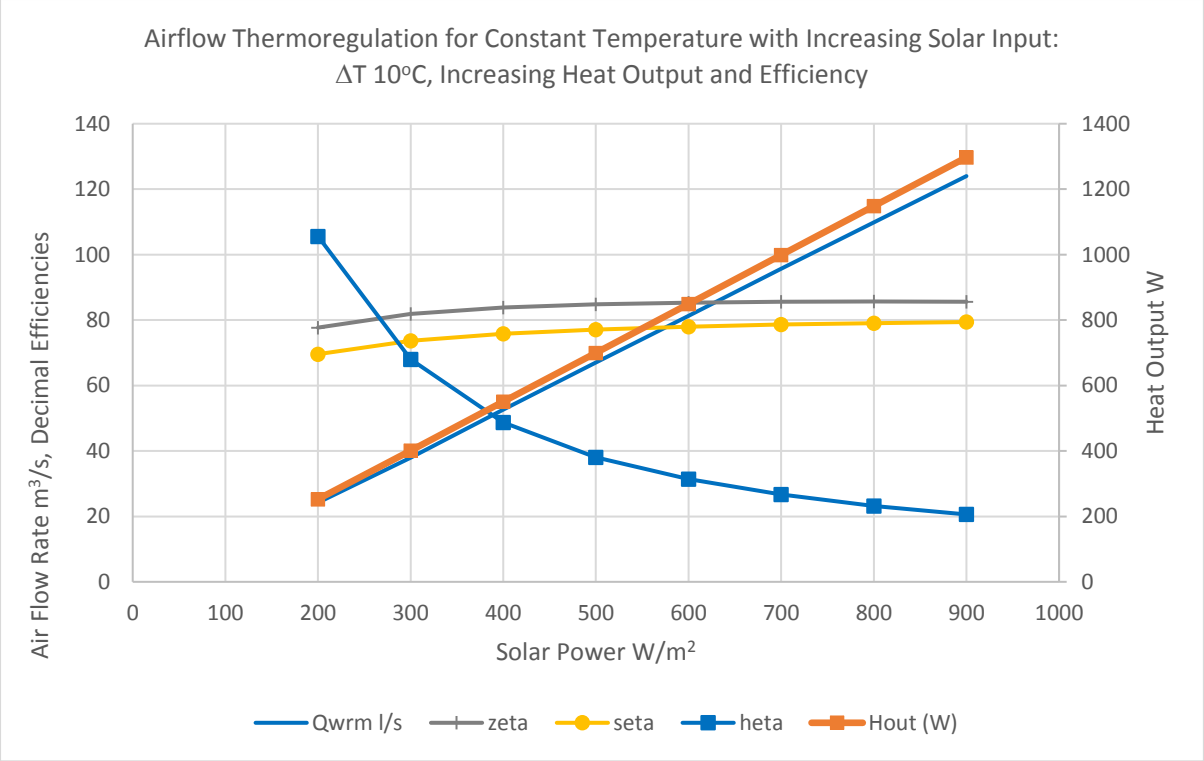

Figure 25: Thermoregulation at ΔT 10oC: increase flow by 15 l/s per 100 W/m2 insolation.

Temperature regulation can thus theoretically be achieved over the full range of solar input. It is relatively difficult to regulate the system for constant heat output: For a given heater power, higher insolation can be reverse-thermoregulated (by the same means, turning down the flow) to maintain the same heater power, however even slightly lower insolation levels cannot be forced to produce significantly higher heater power.

Heater power and efficiency increase with insolation, but fan electrical power is amplified more strongly when the fan is turned down. Amplification is very large in the lowest flow range. Since fan power is the square of flow rate, slow flow costs proportionally less.

This provides a recommendation for the design of thermostat control devices for automated heater operation: As sunlight decreases, an ideal fan power control would gradually turn the flow rate down, then off, and vice versa for increasing sunlight.
If flow rate is held constant, performance tends to improve with insolation. Temperature gain varies from 3 to 15ºC over the 200-900 W/m^2 range, while efficiencies and in particular solar efficiencies are relatively high and vary by less than 10 percent.

Constant Flowrate

Qwrm 0.08 m^3/s

Insolation W/m^2	200	300	400	500	600	700	800	900
ΔT (ºC)	3.1	4.8	6.6	8.4	10.1	11.9	13.8	15.6
Hout (W)	265	411	557	702	847	992	1136	1280
zeta	76.4%	80.9%	83.1%	84.5%	85.4%	86.0%	86.4%	86.7%
seta	73.5%	75.8%	76.9%	77.5%	77.9%	78.2%	78.4%	78.5%
heta	10	16	21	27	32	38	44	49

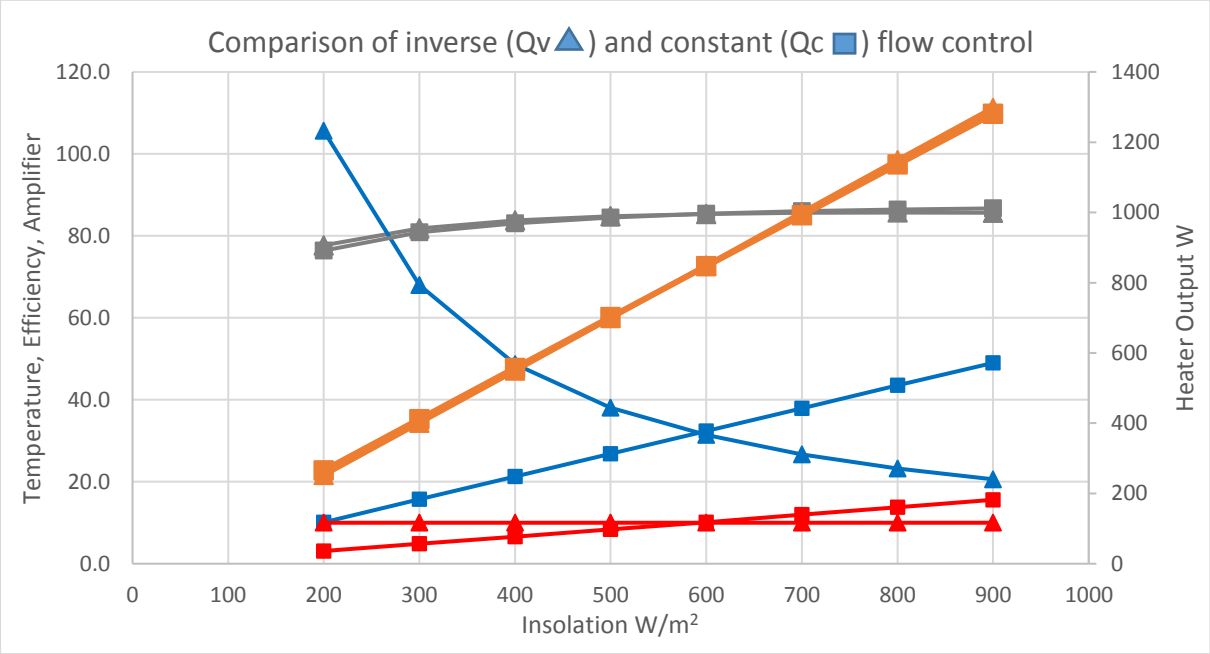

Figure 26: Same colour scheme, comparing constant and thermoregulated operation.

Inverse temperature gains are constant at $\Delta T = 10^o$ while constant flow temperatures increase from 3º to 15º. Heat output and efficency are similar. The key points of difference are the very high amplifier in low-sol Qv and the very poor ΔT in low-sol Qc. Clearly turning the fan down in low-sol weather is important.

Low flow rates perform at consistently higher temperatures and amplification and are more efficient in the low-sol range while not significantly less efficient in the high range: As expected by the fin analysis, heater outputs are only slightly less than at higher flow rates:

Constant Low Flowrate

Qwrm 0.05 m^3/s

Insolation W/m^2	200	300	400	500	600	700	800	900
ΔT (ºC)	5.0	7.7	10.6	13.4	16.3	19.2	22.2	25.3

Hout (W)	264	408	550	693	835	976	1116	1256
zeta	79.0%	82.2%	83.8%	84.6%	85.2%	85.5%	85.7%	85.8%
seta	72.4%	74.6%	75.6%	76.2%	76.5%	76.7%	76.8%	76.8%
heta	26	40	54	68	82	96	109	123

In contrast, high flowrates have lower temperature gains and are not consistently higher in efficiency or significantly higher in heat rate, but are much less efficient in the low insolation range. High flow inefficiencies are due to high fan power relative to solar input. For the same reason the amplification of fan power is much lower.

Constant High Flowrate

Qwrm m^3/s	0.14							
Insolation W/m^2	200	300	400	500	600	700	800	900
ΔT (^oC)	1.8	2.8	3.8	4.8	5.8	6.8	7.8	8.9
Hout (W)	272	420	567	714	862	1009	1155	1302
zeta	67.0%	74.0%	77.8%	80.3%	81.9%	83.2%	84.1%	84.8%
seta	74.2%	76.6%	77.7%	78.4%	78.8%	79.1%	79.4%	79.5%
heta	3	5	7	9	11	13	14	16

Generally high flows should be used only during periods of strong insolation.

Heater output can more than double in 15 minutes if full sun emerges for that time:

12:14 to 12:29 pm on 7 June 2016:
Two consecutive measurements of flow and plate temperatures at 0.099 m^3/s:

	12:14	**12:29**
T_{cold}	11.0	12.0
T_{warm}	16.4	23.7
$T_{plate\ in}$	19.1	26.3
$T_{plate\ out}$	24.7	35.7
ΔT	**5.4**	**11.7**
H_{out} W	**540**	**1164**

This rapid warming was also observed in the continuous temperature series and correlated with an increase in solar temperature via pyranometric thermometer.

Heat Priming

The heater plate can warm to very high temperatures, over 100ºC, if left off in full sun. The heater is then primed with a large reservoir of heat that can be blown off at temperatures of over 50º for several minutes, cooling over 15 minutes with very large net heat flows.

Aluminium has a heat capacity of 910 J/kgK. The plate assembly weighs 37 kg. Cooling from 100ºC to 25ºC the plate releases 2.5 MJ of heat.

The temperature and volume of the resulting warm mix can then be evaluated and set to demand in the house setting. This offers a very rapid warm-up of a house anytime from mid-morning on days of good sun.

Experiment to measure temperatures of outflow and resulting mix temperatures.

14/6/2015 11:30am - 1:30pm: The heater was allowed to warm up for one hour in full sun from an initial shade cover, then blown off at 142 l/s for 20 minutes. Temperatures were recorded every 20 seconds. The final steady state was then extrapolated out to 1 hour.

Initial outflow temperature was recorded at 83.2ºC and cooled over 15 minutes, releasing 0.96 kWh or 3.5 MJ of heat in 130 m^3 of air at an average mix temperature of 40ºC. After one hour the sustained heat flow totalled 1.9 kWh at a mix temperature of 31.5ºC in 511 m^3.

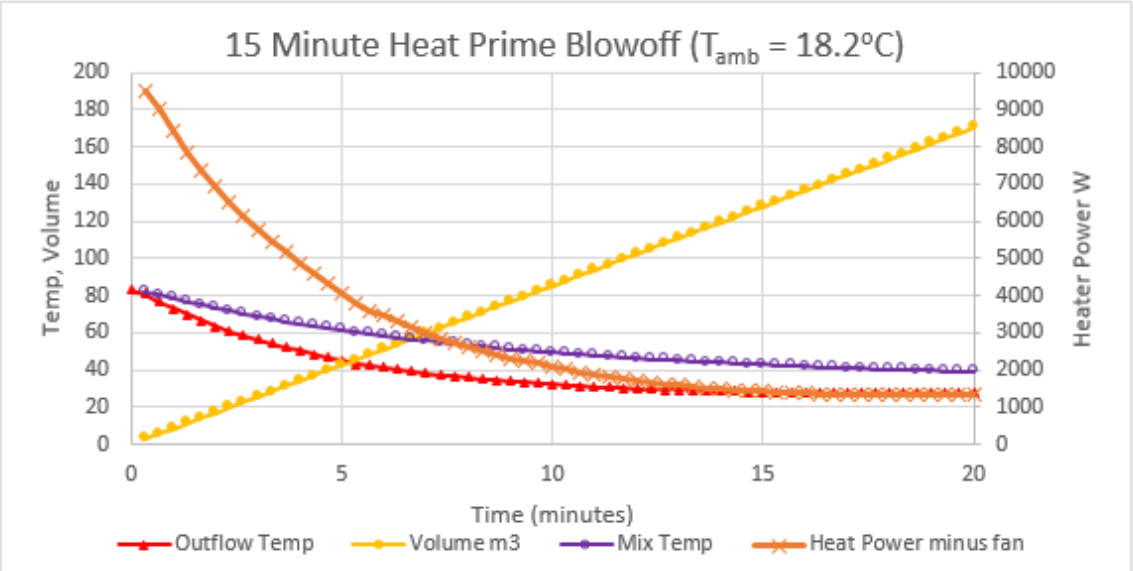

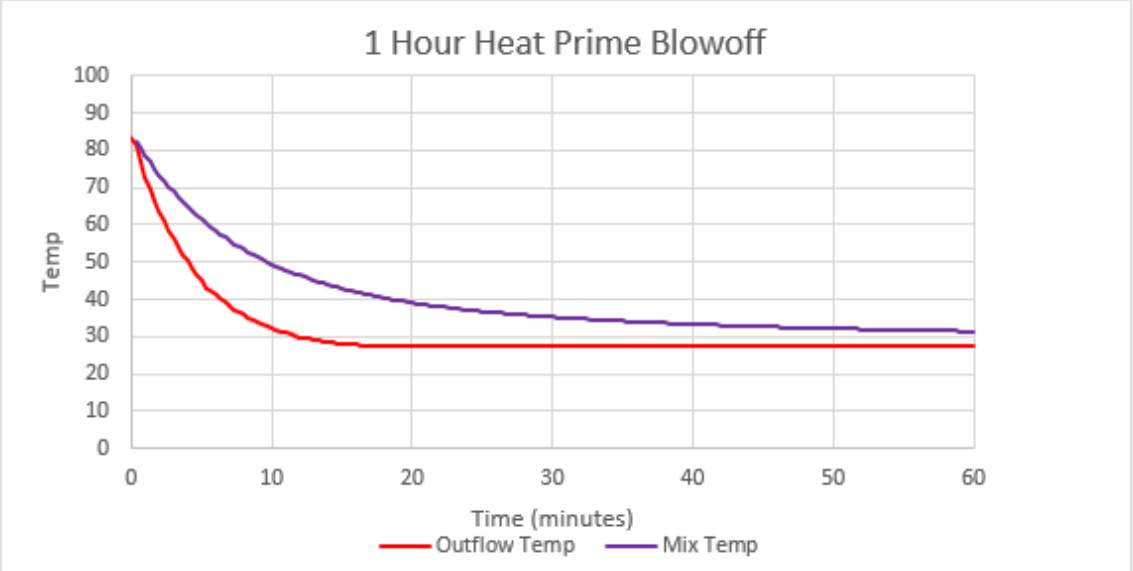

Although performed on a warm winter day, this experiment shows the high power output that the heater can produce, 9.5 kW initially with only 80 W input power, at very large temperature gains. The initial amplification is 120x.

The initial temperature was actually higher than recorded, due to the delay in the thermometer response. This can be seen in the non-Newtonian shape of the graph near $t = 0$.

Average power over one hour is 1.9 kWh/h = 1900 W. That provides an additional 500 W over the steady state power (in the same test) of 1400 W.

This can be regulated to even higher temperatures at only slightly lower flow rates. On a day like this it would be possible to radically warm a 200 sqm house in an hour, to temperatures that will still be warm by late afternoon.

The heater was found to heat to this maximum state of pre-warming in an hour. This mode of operation represents a 2-hour cycle that could be accomplished in the peak 11am-1pm period.

This is an attractive alternative mode of operation for households that are not home in the peak period. With outlet into a laundry drying room, it could revolutionise home heating.

Secondary Heat Flows

Heat is conducted in the direction of any temperature gradient, hence a secondary conduction of heat must occur along the plate from high to low temperature ends. This would have the effect of reducing the temperature difference between those ends and smoothing the distribution of heat flow into and out of the plate.

There must also be a temperature gradient into the plate and along the internal fins of the heat exchanger, since heat conducts from the external to internal plate surface and into the fins before exchanging into the airflow. This suggests that the transfer surface and fin tips of the fins must be cooler than the external plate, altering the heat exchange process.

The accuracy of the theoretical model depends on an order-of-magnitude analysis of these effects. This depends on the relative thermal conductivity of the aluminium plate and fins, which is significantly larger than the turbulent heat transfer coefficient governing the heat exchange process into airflow.

Assuming a constant temperature gradient along the plate, heat conduction along the gradient will also be constant:

$$Q = k.A.dT/dx$$

where k = 205 W/mK, the thermal conductivity of aluminium and A (patent information) is the cross-sectional area of the aluminium plate. dT/dx is typically 10 ^{o}C/m. This gives an estimated heat flow of 14 W *back* along the plate, which is a small proportion of operating heat flow through the plate.

Similarly a temperature difference must exist between the external and internal plate surfaces: expressing the same equation in W/m^2, typically a heat exchange of 600 W/m^2 as experimentally measured, the temperature gradient into the plate is

$$dT/dx = 600/205 = 2.9\ ^{o}\text{C/m}$$

The plate depth (patent) gives a temperature difference of approximately 0.01 ^{o}C between external and internal plate surfaces.

Fin cooling is controlled by the conduction of heat along each fin. Airflow is channeled between pairs of fins which can be bisected along their centrelines and added together to

represent the same heat flow as a single fin. This heat is estimated by net external heat absorption minus re-radiation, and reduced by the proportion of heat exchanged directly from the internal surface:

Heat Inflow to Fin = $(aI - 1.05e\sigma(\text{average}(T_p^4) - T_a^4)).(w_c + t_f).L - h(T_p - T_a).w_c.L$

or $Q_f.L = Q_i.L - Q_o.L$

where w_c and t_f are the channel width and fin thickness. Because of the constant temperature gradient and constant plate-air temperature difference this can be evaluated per length of plate, ie the plate length L cancels.

Heat conduction along the fin reduces with depth as heat is exchanged into the flow. Assuming a nearly constant rate of heat exchange per length, which implies a nearly constant fin temperature, the heat flow rate and temperature gradient are linear:

$$Q_f = (Q_i - Q_o)(1 - y/D) = k.(dT/dy).t_f$$

where D is the fin depth. This can be integrated directly, deriving an integration constant of T_p at $y = 0$:

$$T = T_p - (Q_i - Q_o)/(kt_f).(y - y^2/2D)$$

At typical (50%) operation, net absorption minus re-radiation into the plate is 1100 W. The channel width, fin thickness (pending patent information) and emission area reduce this to 10.8 W/m heat flow into each channel. Of this, 1.4 W/m are exchanged directly from the internal plate surface in each channel. Hence $(Q_i - Q_o)$ = 9.4 W/m.

At the fin tip, $y = D$ hence $(y - y^2/2D) = D/2$. Given k = 205 W/mK and the patent fin thickness, the resulting fin temperature differential is 0.7°C. This analysis was repeated at a second order approximation with no assumptions regarding linearity of the heat flow gradient, with similar results, in fact the second order heat profile within the fin is indistinguishable visually from a simple straight line.

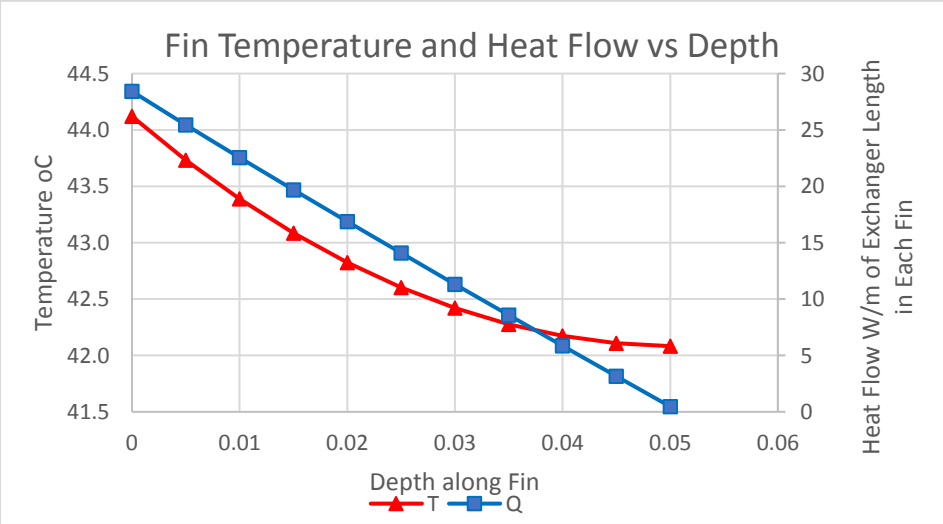

It is evident that for typical operating conditions the fin is very nearly the same temperature along its length, cooling by only 0.7 °C at the tip. The resulting heat exchange capacity of the

fin is approximately 97.4% of the full capacity assuming external plate temperature. Applying this factor to the model has a negligible effect on output, easily corrected by a 10 W/m^2 adjustment of net absorption with no change to the heat transfer coefficient.

The three effects examined here are found to have a combined error of 3%. All characteristic graphs presented above have the corrections for fin temperature and through-plate conduction included.

From the above it can be concluded that these secondary effects due to heat flow are negligible and the model's precision should be well within experimental error for ideal uniform-constant conditions. Empirical errors due to measurement and local conditions are generally larger than these theoretical corrections.

Fin Design Analysis

Modelling the system over a range of flow rates and fin spacings reveals an optimal fin density with regard to heat exchange performance. This mirrors the conclusions of the original design process based on more advanced numerical modelling.

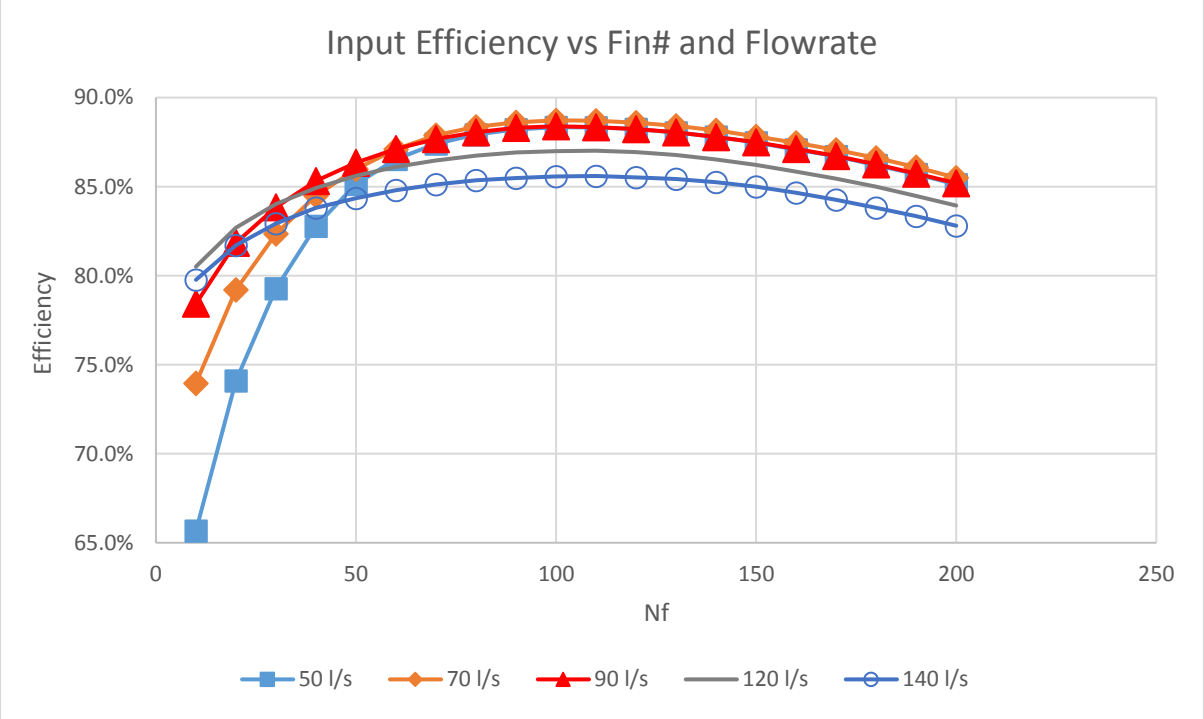

The complex intersection of efficiencies around *Nf* = 54 (a design parameter, the "fin number") indicates a region in which efficiencies are relatively constant for varying flowrate. This is regarded as an optimal point, giving an economically low *Nf* and reasonably high efficiences (around 86 – 87%) which are nearly equal at all flow rates. This point of reliable and effective operation corresponds to the parameter adopted in the Solrheat design.

The fin spacing design was based on these thermodynamic optima, as well as practical construction aspects such as extrusion process technology and overall weight of the panel. A "comb" design would have over half the mass of a 50 mm aluminium plate. The thermally optimal fin number *Nf* = 100 does nor provide much more efficiency (from 87.1% to 88.4%) but significantly increases construction costs.